TITLE: # 4K Reference Load 30 GHz RCA Test Report

DOC. TYPE: REPORT

PROJECT REF.: PL-LFI-TES-RP-004 **PAGE:** I of V, 43

ISSUE/REV.: 1.0 **DATE:** November 8th, 2004

Prepared by	**L. TERENZI** **LFI 4K Load Development Team** **F. CUTTAIA** **LFI 4K Load Development Team** **A. DE ROSA** **LFI 4K Load Development Team**	**Date:** **Signature:**	November 8th, 2004
Agreed by	**L. VALENZIANO** **LFI Project System Team**	**Date:** **Signature:**	**November 8th, 2004**
Approved by	**N. MANDOLESI** **LFI** **Principal Investigator**	**Date:** **Signature:**	November 8th, 2004

DISTRIBUTION LIST

Recipient	Company / Institute		Sent
J. MARTI-CANALES	ESA – Noordwijk	Javier.Marti.Canales@esa.int	Yes
N. MANDOLESI	IASF – Sezione di Bologna	reno@tesre.bo.cnr.it	Yes
C. BUTLER	IASF – Sezione di Bologna	butler@tesre.bo.cnr.it	Yes
M. BERSANELLI	Unimi – Milano	Marco.Bersanelli@uni.mi.astro.it	Yes
L. TERENZI	IASF – Sezione di Bologna	lteren@bo.iasf.cnr.it	Yes
F. CUTTAIA	IASF – Sezione di Bologna	cuttaia@bo.iasf.cnr.it	Yes
LFI System PCC	IASF – Bologna	lfispcc@bo.iasf.cnr.it	Yes

CHANGE RECORD

Issue	Date	Sheet	Description of Change	Release
0.1	August,10,'04	All	First issue of this document	
1.0	November,8,'04	All	RF results and dimensional verification added	

TABLE OF CONTENTS

1 INTRODUCTION

1.1 Purpose

Tests are devoted to verify the RCA 30 GHz 4KRL compliance with requirements described in RD**. Dimensional verifications, joined with thermal and radiometric analysis, are then required.
Each part is dimensionally characterized by evaluating its size and weight. A radiometric measure is performed on passive devices (Reference horns) separately and combined with the reference loads to characterize them before thermally cycling in a cryo-facility. Thermal cycles have a double scope: to apply a thermal stress to the samples, in order to verify their mechanical resistance to cryogenic temperature; to verify the thermal transfer from the reference temperature link (the cryo-cooler cool flange) to the reference load surface facing the reference horn.
A second set of radiometric measurements is performed after the last thermal cycle to compare starting and final performances: radiometric comparison, if measurements get compatible results, allows to state that no modification in the mechanical properties is produced by thermal cycling. The compliance with RF requirements is then tested.

1.2 Document Overview

The test flow is presented in §2.
A brief description of the parts under test is given in §0, together with the detailed designs, reported in section §3.3. The thermal test is described in §5, focusing on measurement set-up and instrumentation (§5.1), thermal curves (§5.3), visual inspections. Radiometric measurements are presented before and after the thermal cycling in §4 and §6 in order to check changes due to it: comparison test (§6.1) and (§6.2) and requirements verification tests (§7) are shown giving details on instrumentation employed (§7.1) , on experimental setup and on results (§8). Conclusions are given in §9

1.3 TERMS and ACRONYMS

4K RL	4K Reference Load
FEM	Front End Module
FM	Flight Model
I/F	Interface
IL	Insertion Loss
LFI	Low Frequency Instrument
MS	Mounting Structure
N/A	Not Applicable
QM	Qualification Model
RH	Reference Horn
RL	Return Loss
RT	Reference Target

TBC	To Be Confirmed
TBD	To Be Defined
TBR	To Be Refined
TBI	To Be Included
RLSy	Reference Load System

1.4 APPLICABLE AND REFERENCE DOCUMENTS

REF[1] F. Cuttaia, *'4K Reference Load RF Test Procedures'*, PL-LFI-PS-PR-001, 2004
REF[2] F. Cuttaia, *'Optimization of the 4K Reference Load in the LFI 70GHz band*, PL-LFI-TES-RP-002, 2003
REF[3] L. Valenziano, '*4K Reference Load requirement Specification'*, PL-LFI-TES-SP-001
REF[4] 70GHz Reference Load drawings
REF[5] 70GHz Reference Horn drawings
REF[6] LakeShore Cryotronics inc. Model 340 user's manual

2 Test Flow

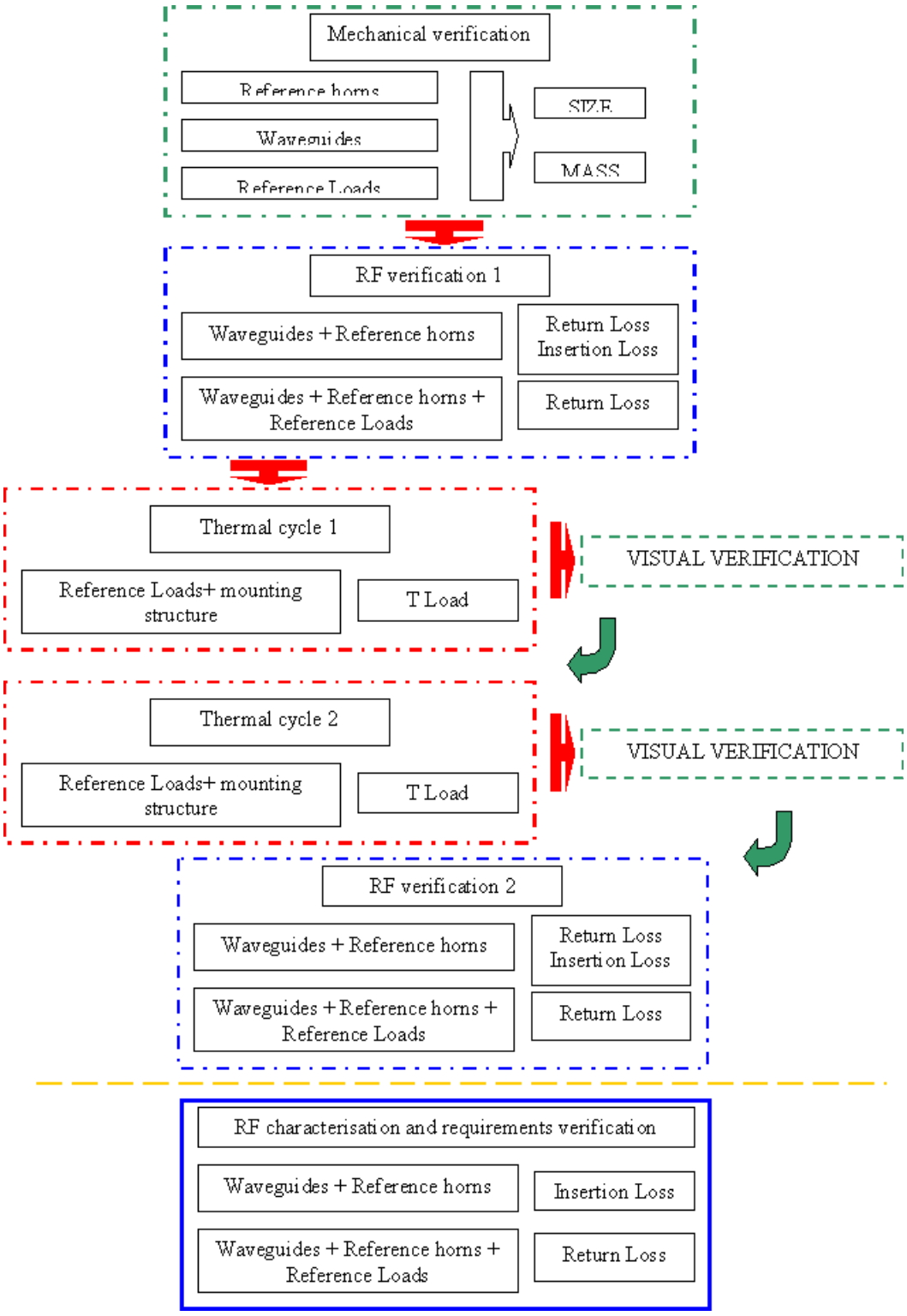
Mechanical verification
Reference horns
Waveguides
Reference Loads
SIZE
MASS
RF verification 1
Waveguides + Reference horns
Return Loss
Insertion Loss
Waveguides + Reference horns + Reference Loads
Return Loss
Thermal cycle 1
Reference Loads+ mounting structure
T Load
VISUAL VERIFICATION
Thermal cycle 2
Reference Loads+ mounting structure
T Load
VISUAL VERIFICATION
RF verification 2
Waveguides + Reference horns
Return Loss
Insertion Loss
Waveguides + Reference horns + Reference Loads
Return Loss
RF characterisation and requirements verification
Waveguides + Reference horns
Insertion Loss
Waveguides + Reference horns + Reference Loads
Return Loss

3 MECHANICAL DESCRIPTION

3.1 Parts identification

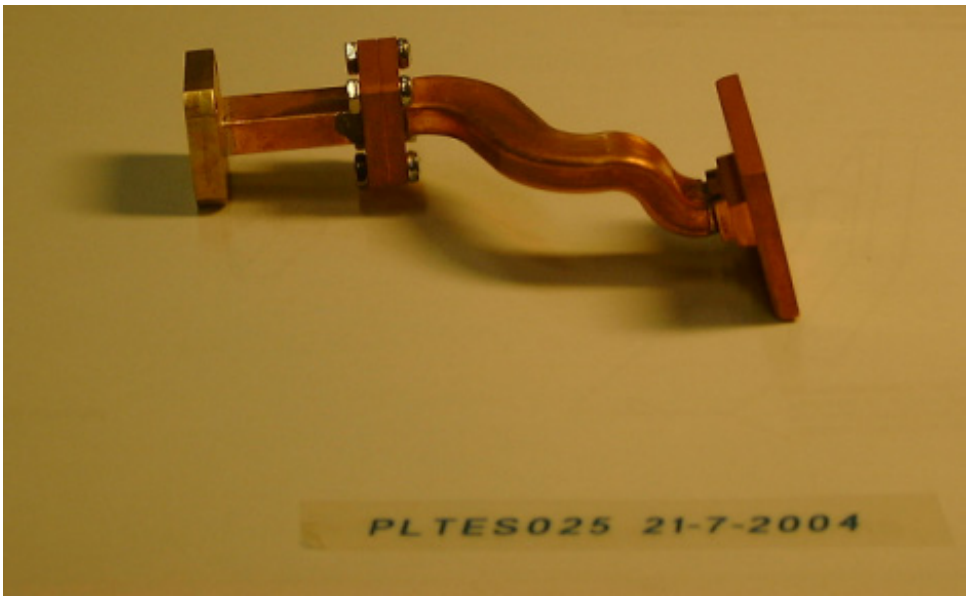

Fig. 1 Waveguide and Reference Horn 28L (id:PL-TES-025)

Fig. 2 Waveguide and Reference Horn 28L (id:PL-TES-025)

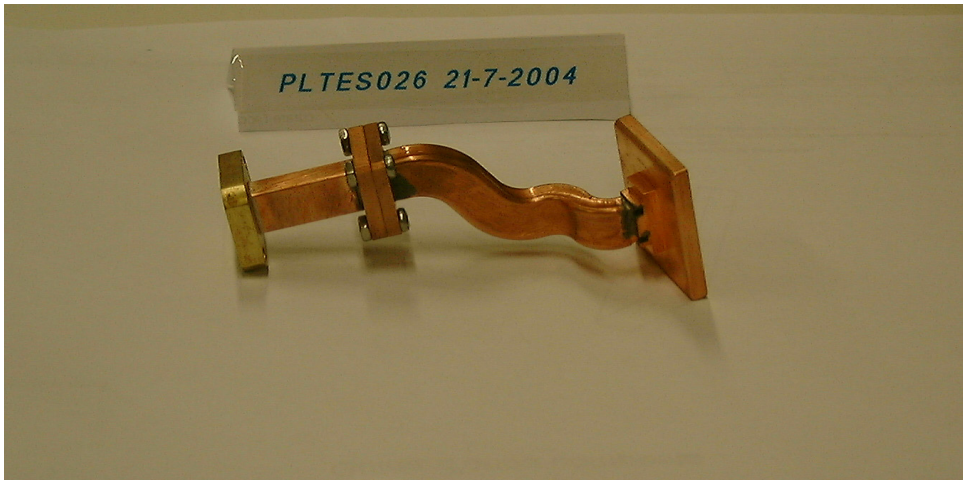

Fig. 3 Waveguide and Reference Horn 28R (id:PL-TES-026)

Fig. 4 Waveguide and Reference Horn 28R (id:PL-TES-026)

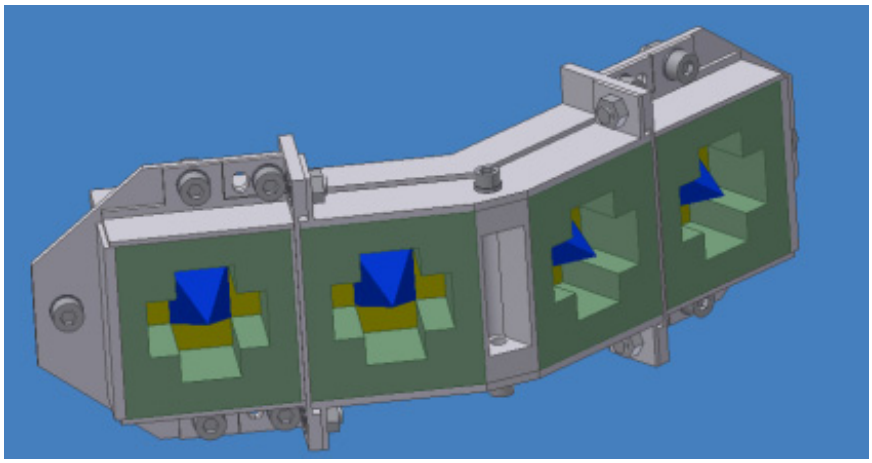

Fig. 5 4K Reference Loads (the fourth reference load- starting from the left- is not present in the device under test)

3.2 Design

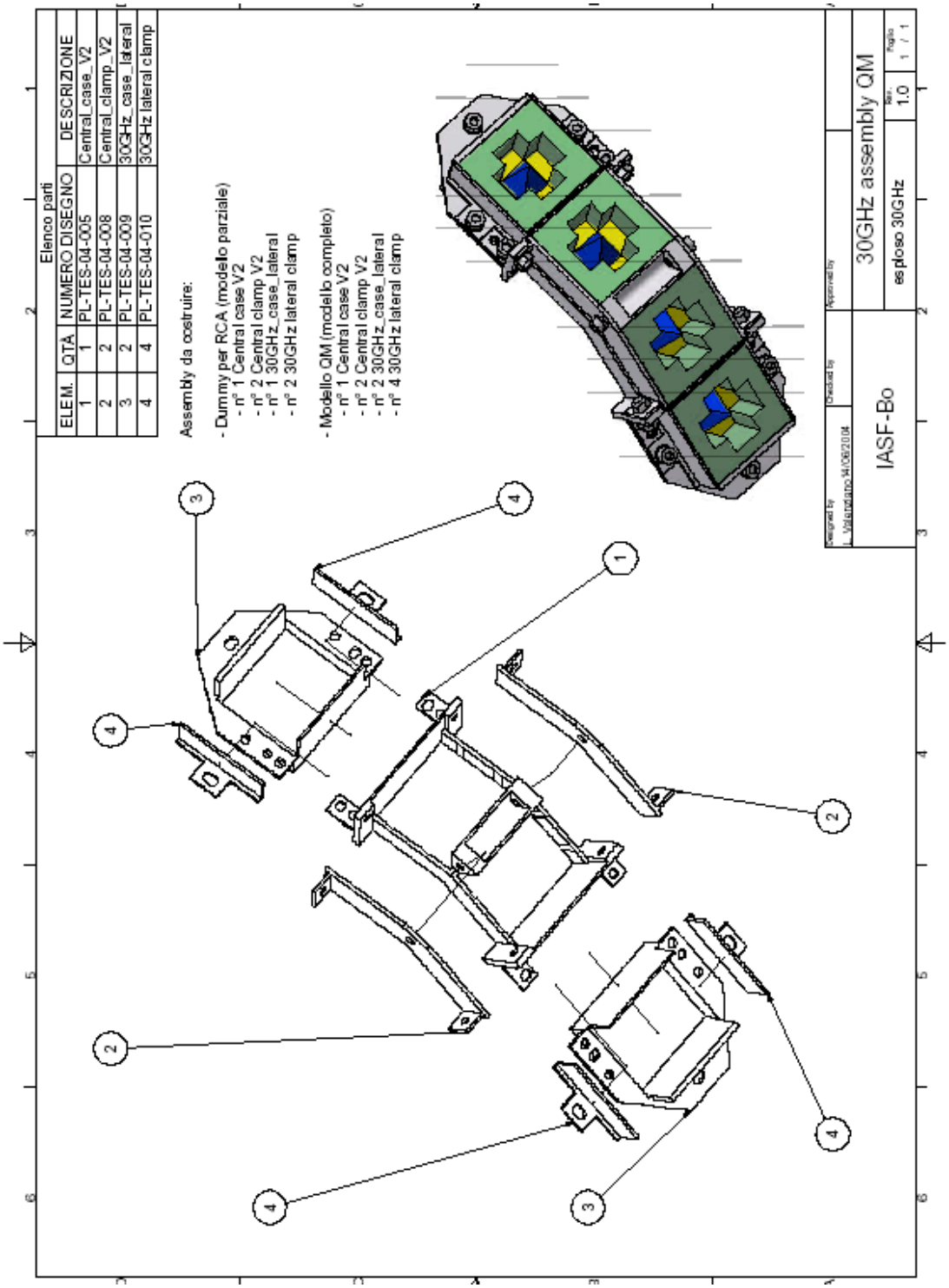
Elenco parti
ELEM. | QTÀ | NUMERO DISEGNO | DESCRIZIONE
1 | 1 | PL-TES-04-005 | Central_case_V2
2 | 2 | PL-TES-04-008 | Central_clamp_V2
3 | 2 | PL-TES-04-009 | 30GHz_case_lateral
4 | 4 | PL-TES-04-010 | 30GHz lateral clamp
Assembly da costruire:
- Dummy per RCA (modello parziale)
- n° 1 Central case V2
- n° 2 Central clamp V2
- n° 1 30GHz_case_lateral
- n° 2 30GHz lateral clamp
- Modello QM (modello completo)
- n° 1 Central case V2
- n° 2 Central clamp V2
- n° 2 30GHz_case_lateral
- n° 4 30GHz lateral clamp
Designed by
L.Valenziano 14/06/2004
Checked by
Approved by
IASF-Bo
30GHz assembly QM
esploso 30GHz
Rev.
1.0
Pagina
1 / 1

3.3 Waveguides dimensional verification

3.3.1 Size

Dimensions of parts PL-TES-025 and PL-TES-026 have been measured by using a milling machine provided with a feeler pin. Final dimensions of part PL-TES-025 after the second machining were measured by 'Officine Pasquali' by using a DEA dimensional measurements system.

Nominal and measured dimensions are reported below. Dimensions of part PL-TES-026 reported in table ** refer to the IASF-Bo measurement; dimensions of part PL-TES-025 refer to the Officine Pasquali measurement after the last machining (in fact the part was then directly delivered to Laben S.p.a. by Officine Pasquali)

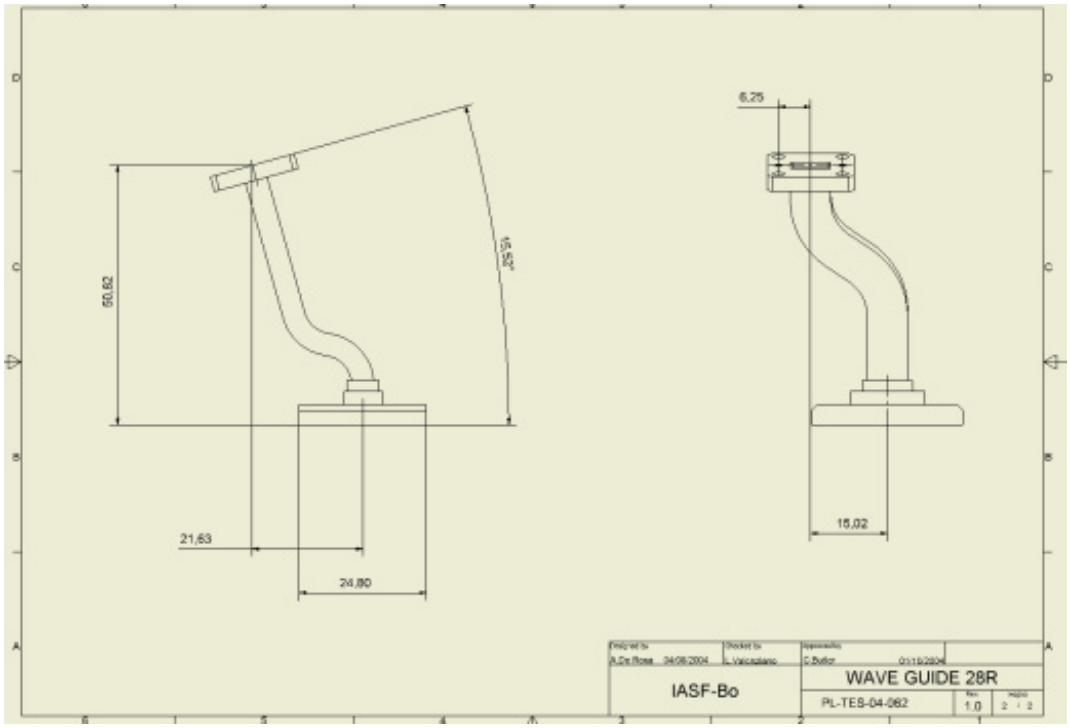

Figure 1 Nominal dimensions for part PL-TES-025

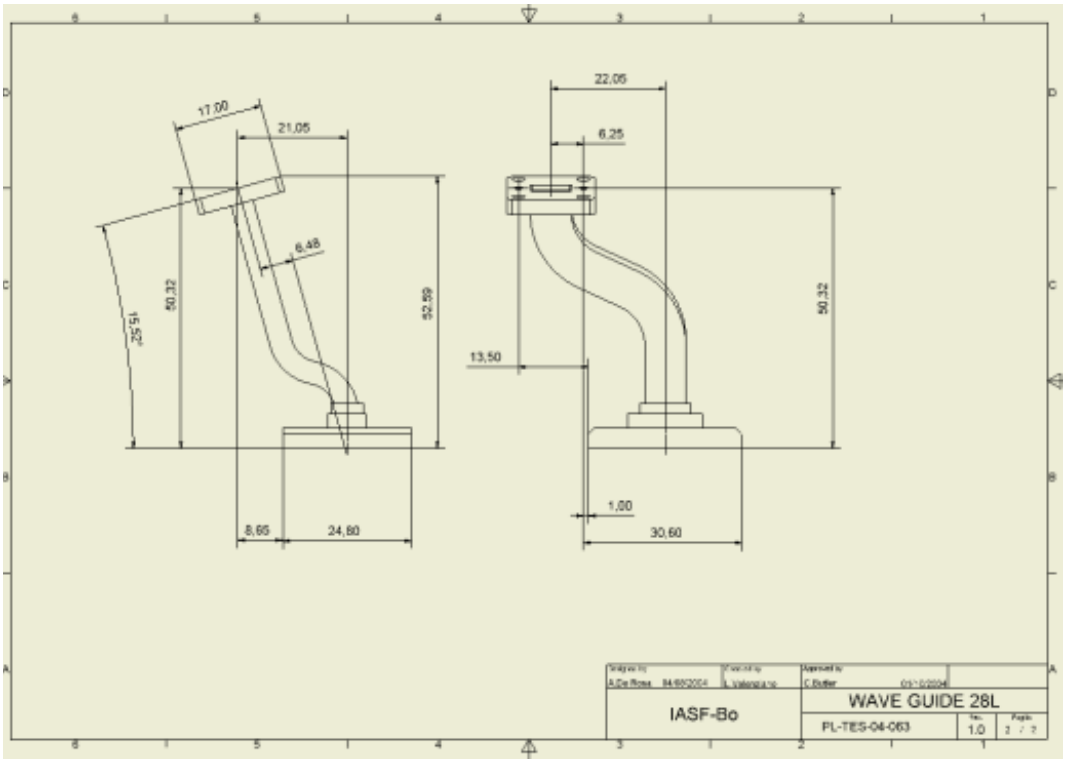

Figure 2 Nominal dimensions for part PL-TES-026

Axis	Nominal	Measured	Dev
x	-22.050	-22.306	+0.256
y	21.050	22.014	+0.964
z	50.320	49.255	-1.065
Angle	15.520	16.507	+0.987

Table 1 measured dimensions (OP) for the part PL-TES-025 after the second machining.

Angle	15.520	16.12	+0.60
	0	0.45	+0.45

Table 2 measured dimensions (IASF) for the part PL-TES-026 .

3.3.2 Mass

The two parts have been weighted by using a precision digital balance. A table reporting comparison between nominal and taken data follows.

Axis	Nominal	Measured	Dev
PLTES025	27.14	32.81	-5.67
PLTES026	26.85	32.81	-5.96

Table 3 comparison between nominal and measured weights.

3.3.3 Notes

The visual and dimensional inspection of the part PL-TES-026 showed its non-conformity with the design. In fact the first H-plane bend was found curved in the opposite direction respect to the project. This difference does not modify the RF performances but however avoids the correct mounting in front of the corresponding Reference Load. This relevance imposed to machine again the part in order to make safe the original design.

4 Thermal stress resistance verification by RF measurements

4.1 Measurement philosophy

The scope is that of verify the integrity of each reference target allocated inside the mounting structure by testing its radiometric behavior before and after the thermal cycles.
The figure of merit set to investigate these features is the Return Loss evaluated in the whole WR28 range (26,5 GHz – 40 GHz); in fact it is supposed that some break o detachment, due to the thermal contraction, inside the reference load, should correspond to a variation in the electrical properties of the load. Moreover, being the power detected by the LFI radiometers nothing else than the integrated power of the thermal distribution, over the operative frequency, convolved with the antenna pattern, if no change in the reflectivity and in the thermal properties of the load is registered after the thermal cycles, it means that the sample is not damaged or modified, at least in its features of our interest.

4.2 Instrumental setup

A reference test EBB antenna was employed to make the measurement. In fact it has a response very close to the one expected from the QM Reference horn and moreover has a peculiar return loss lower than the QM model, where a degradation, also if little, is due to the waveguide mismatching. It allows us to appreciate also little variations due to any hardware modification in the Load structure. The instrumentation employed is composed of:

- A Vector Network Analyzer working from 26,5 GHz up to 40 GHz.
- A Test pyramidal horn antenna working from 26,5 GHz up to 40 GHz.
- A metric bench provided with digital manipulators allowing translations along three axis and rotations around the vertical axis.
- A mounting structure holding the case lodging the reference loads.

The instrumental assembly is presented in detail in Fig. 6.

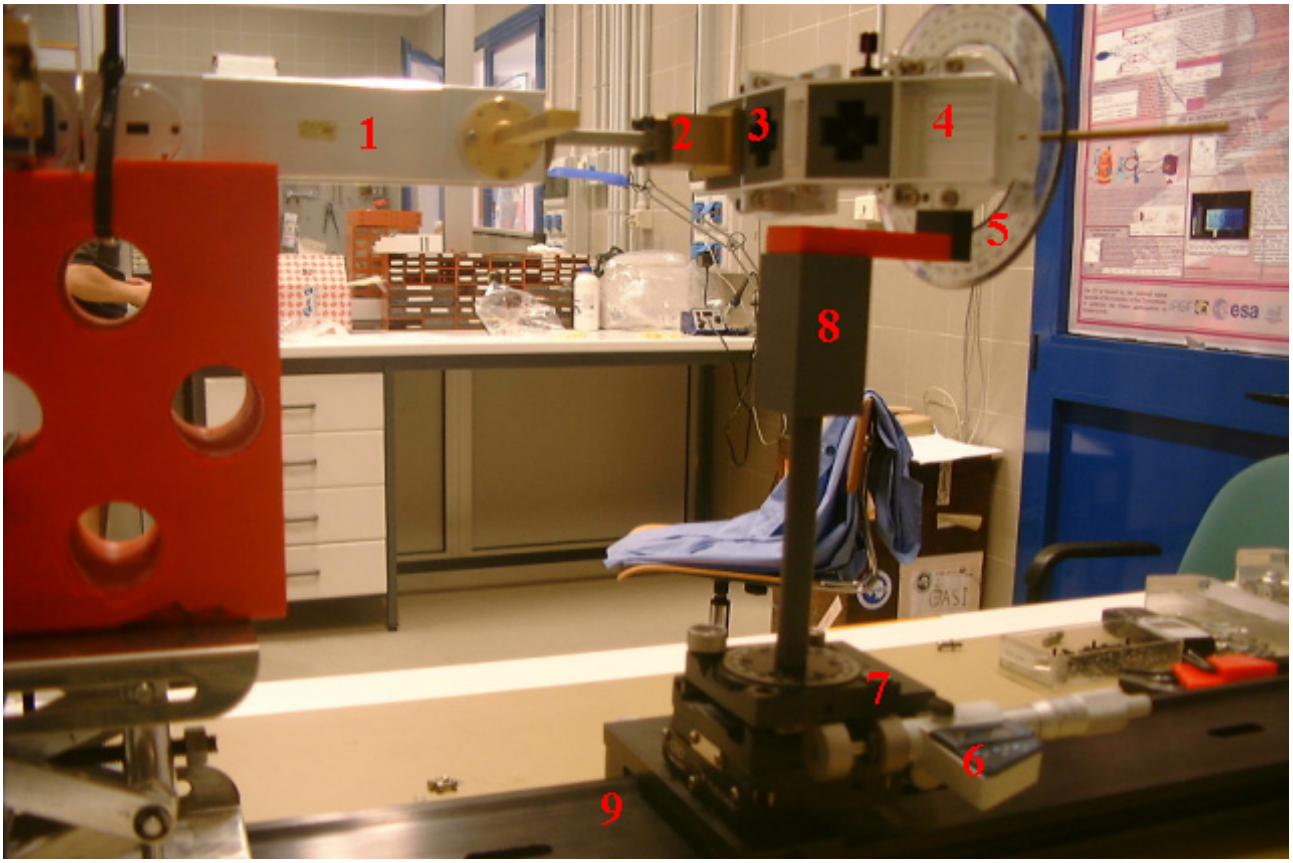

Fig. 6 instrumental setup for the thermal stress resistance RF verification: 2) VNA Head transmitter; 3) test horn; 3) DUT (three reference loads) ; 4) 4KRL mounting case; 5) rotational stage; 6) linear manipulators with digital display; 7) rotational manipulator; 8) mounting support; 9) optical bench.

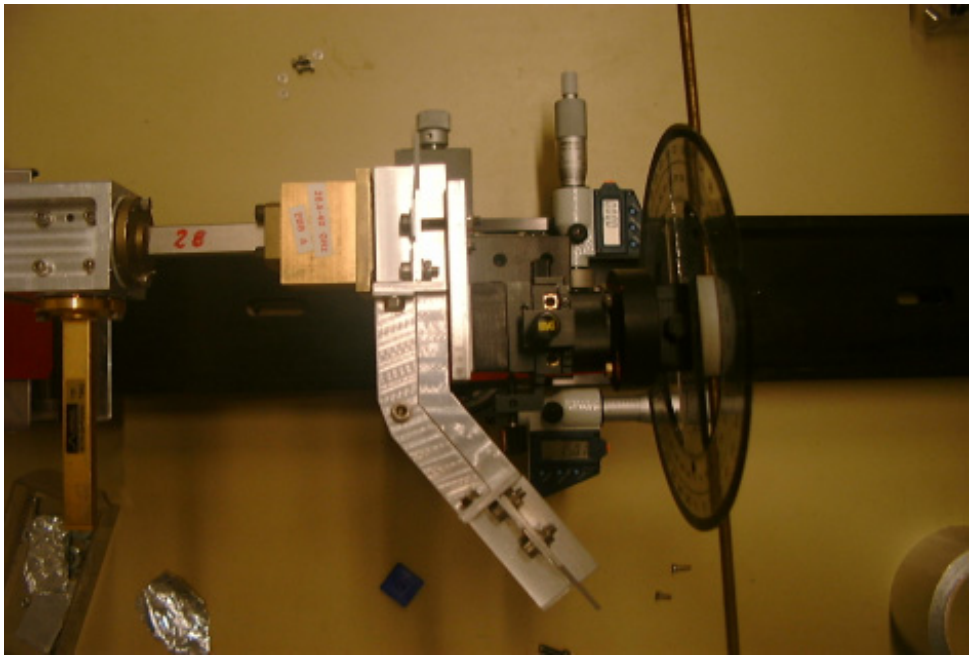

Fig. 7 measurement setup top view

Fig. 8 VNA panel

4.3 Starting performance verification

The Return Loss of the system Test EBBA Horn + Reference Target was measured, before the first thermal cycling, at the nominal distance of 1,5 mm. The same horn was employed to test the three reference loads. Results are presented in section §6.1 compared with data taken after the thermal cycles.

5 Thermal Tests

5.1 Test setup

Test is performed in the IASF-Bo 4K cryo facility, fully described in RD 2. Parts are manufactured by Officine Pasquali and delivered to IASF.

5.1.1 Temperature sensor characteristics

The temperature sensors used are LakeShore DT670 silicon diode and CX-1050 cernox RTDs; the accuracy of uncalibrated diodes is ±0.25K at 4 K, while for calibrated diodes and cernox is 20 mK and 5 mK respectively at temperatures lower than 10 K, as reported in REF[6] .

Sensors are read by means of a LakeShore temperature controller model 340, which, at 4 K, reads out temperature with a sensitivity of 0.4 mK for silicon diodes and 0.1 mK for Cernox resistances.

5.2 Sample preparation

The sample consists of the 30 GHz unit of the Planck LFI 4K reference load, consisting of three targets, from four nominal, with their cases and Aluminum support structure. Two copper supports
provide the interface to the cryo facility cold flange.

5.2.1 Preliminary inspection of the parts

The sample was inspected before mounting it in the cryofacility.
No crack is observed, no flaking is observed.

5.2.2 Sample mounting

Sample parts are cleaned with alcohol. Copper support were screwed to the facility cold flange providing both thermal contact and mechanical support (see). Temperature sensors were mounted on the cold flange and on the interface between Aluminum support structure and copper, as reported in Table 4.

Sensor ID	**Type**	**Fixation**	**Location**
A	DT670 SD (cal)	Al tape	Target outer face
B	Cernox CX 1050 (cal)	Screw	Interface with copper support
C1	DT670 CU	Screw	Cold flange

Table 4 Sensor location for the thermal cycles.

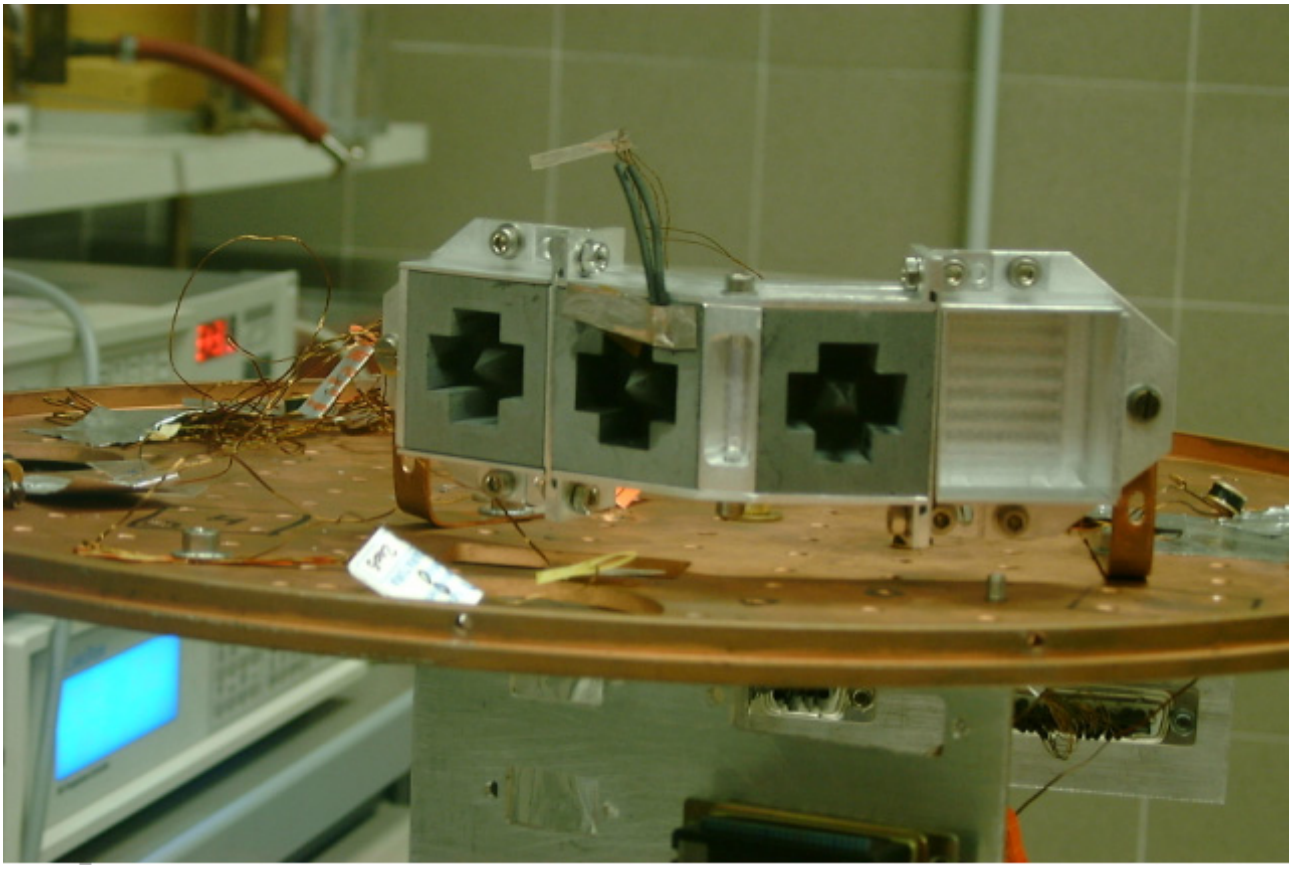

Figure 3

5.3 Thermal cycles

5.3.1 Cycle 1

The test started on July, 19th, 2004 at 15:00. The CF was evacuated using a dry rotative pump. When a pressure of 6.0E-2 mbar was reached, the cooler was started at 18:10. Acquisition of temperature sensors was started at 18:10 on July, 19th. Acquisition period was set to 60s. The pump was stopped when the pressure reached 1.3E-2 mbar. Cool-down data are reported in Figure 4 and Figure 5.

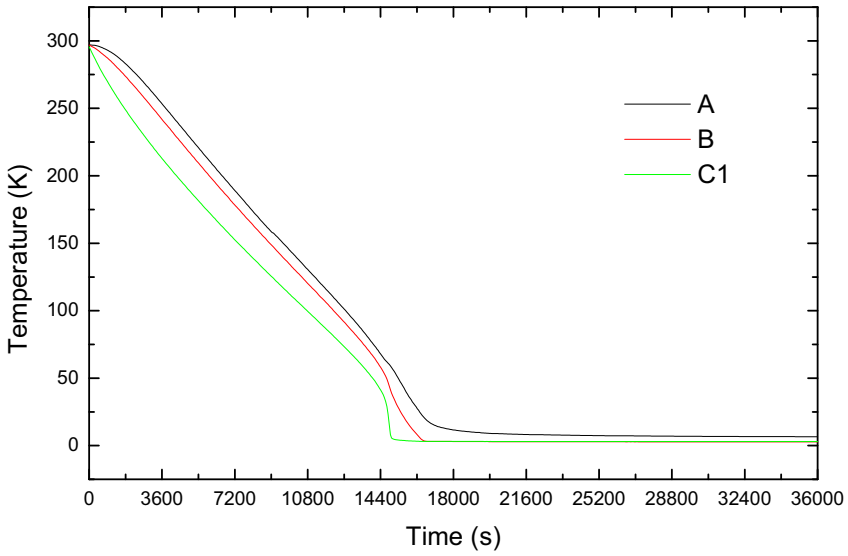

Figure 4 Cooldown curves for the first cycle

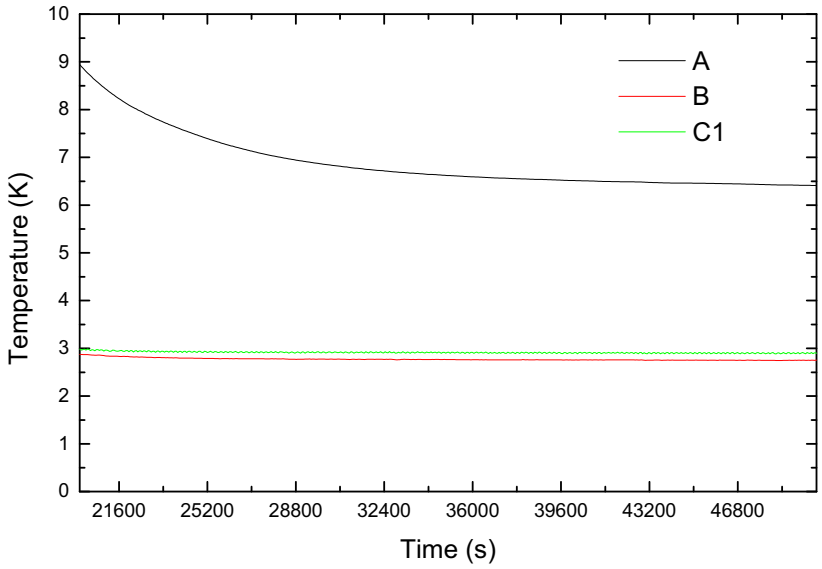

Figure 5 Detailed view of low temperature thermalization during the first cycle. As evident, sensors A temperature is much higher than the other ones.

The A sensor has thermalized at a quite high temperature of about 6.5 K.
On July 20th, 2004, the cryocooler was turned off at 9:40. Warm-up procedure was started. Additional heating (about 9 W) was introduced using resistors mounted on the cold flange.

Once the temperature of 287K was reached by the reference sensor (A), the CF was filled with dry air and opened.

Temperature sensors A were found slightly detached from the sample, due to Al tape low adherence caused by Apiezon thermal grease contamination. All other sensors were still in place and appeared in good physical contact with the sample. Sensor location was re-checked.

5.3.2 Inspection 1

Pictures were taken and no damage, crack or detachment was found

5.3.3 Cycle 2

All parts in their contact surfaces were cleaned with ethylic alcohol.
The sample was re-mounted in the CF. Temperature sensors were mounted as for the first cycle (Table 4).
This time A sensor was mounted without Apiezon N grease.

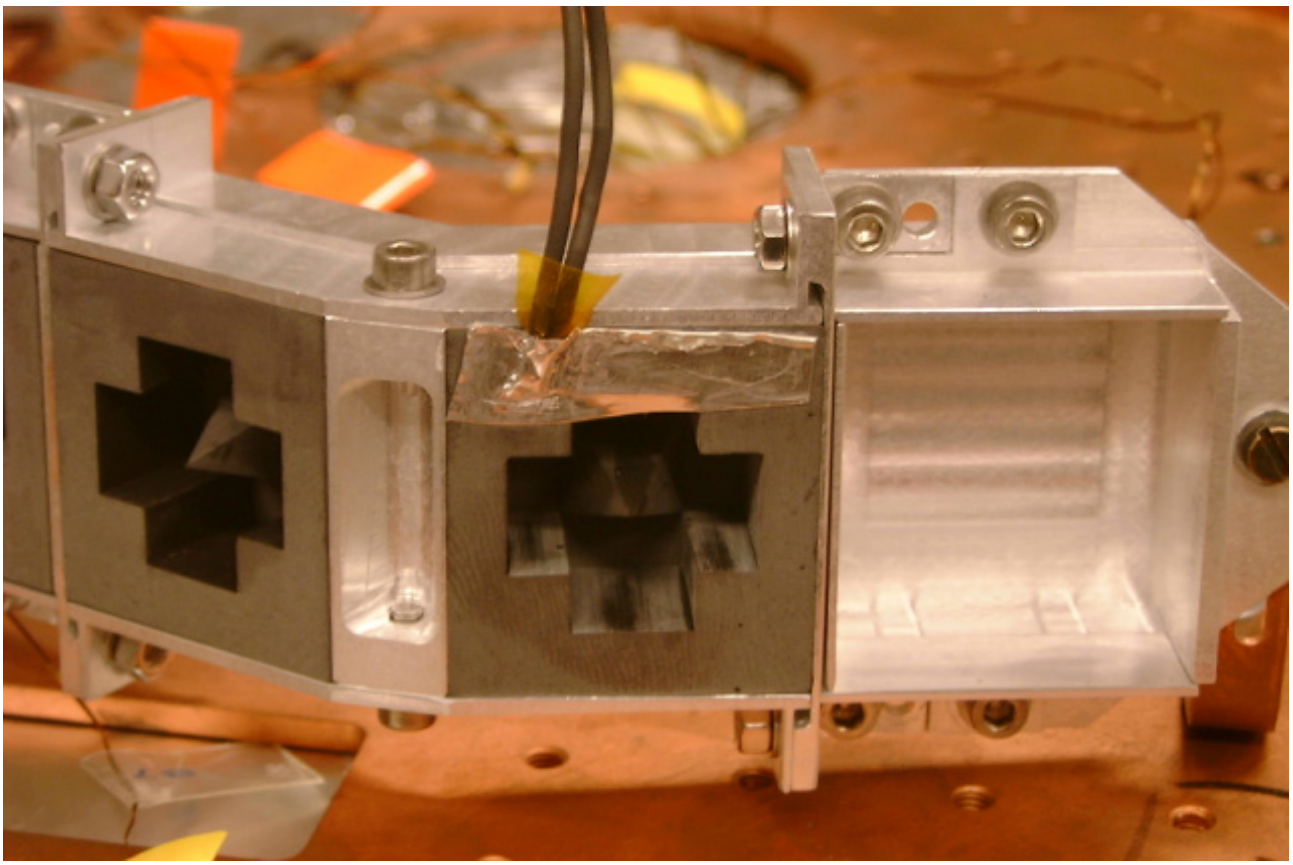

Figure 6

In the following figures cooldown curve for the second cycle is reported.

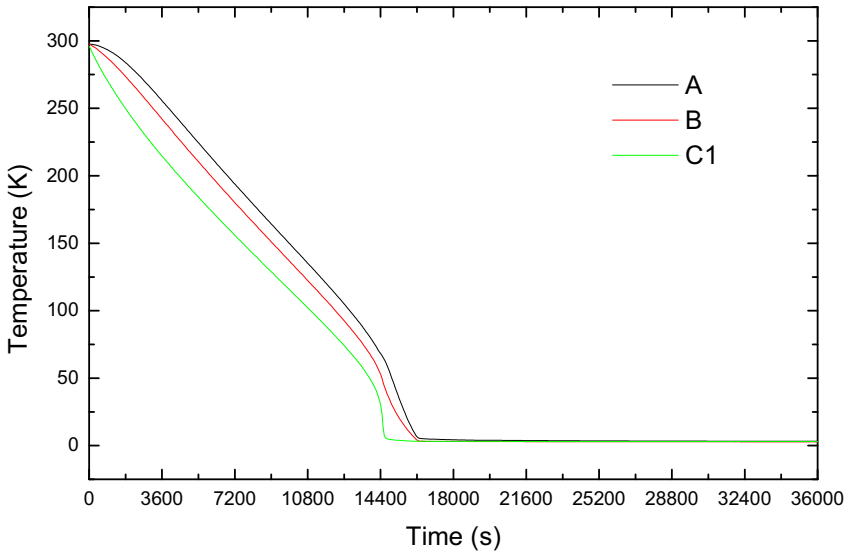

Figure 7 Cooldown curves for cycle 2.

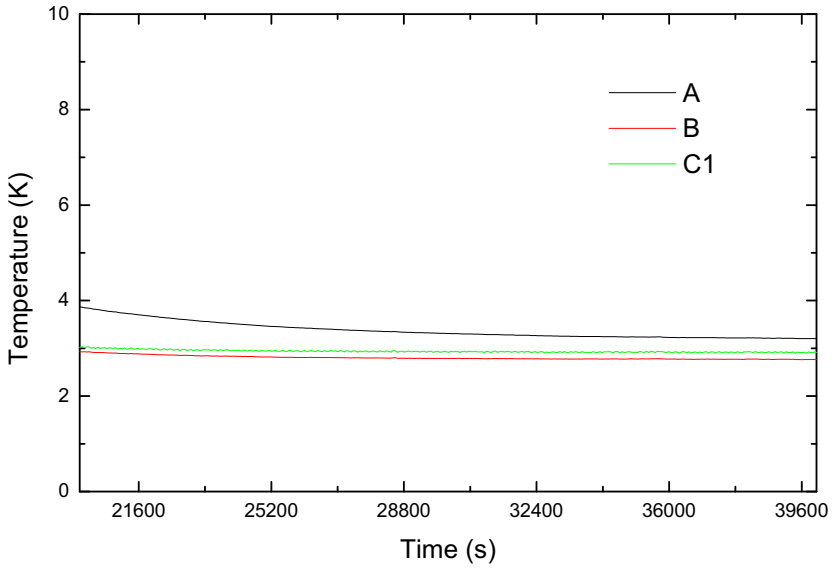

Figure 8 Temperature curves of the cycle 2 thermalization; this time sensor A has thermalized at about the same temperature of other sensors

5.3.4 Inspection 2

After the warm up the CF was air filled and opened. The sample did not present any problem, crack or detachment.

6 Final performance verification

The same tests described in §4 have been performed after the last thermal cycle. Results and comparisons are presented in the next paragraph.

6.1 Data analysis

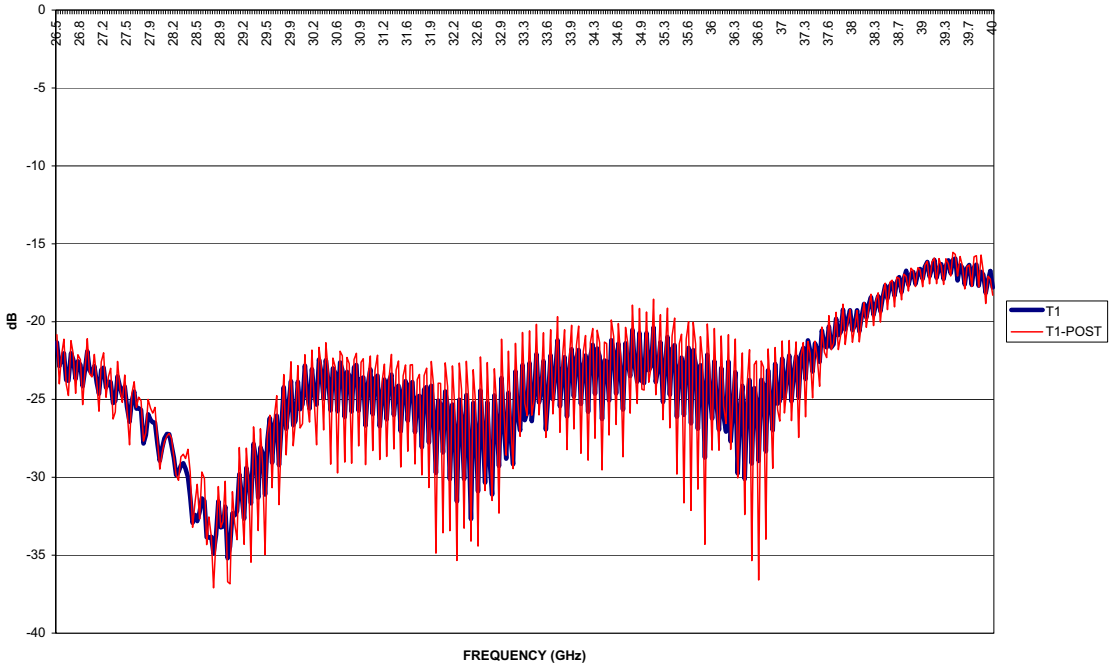

Figure 9 Target 1 Return Loss amplitude comparison before (blue line) and after (red line) thermal cycling.

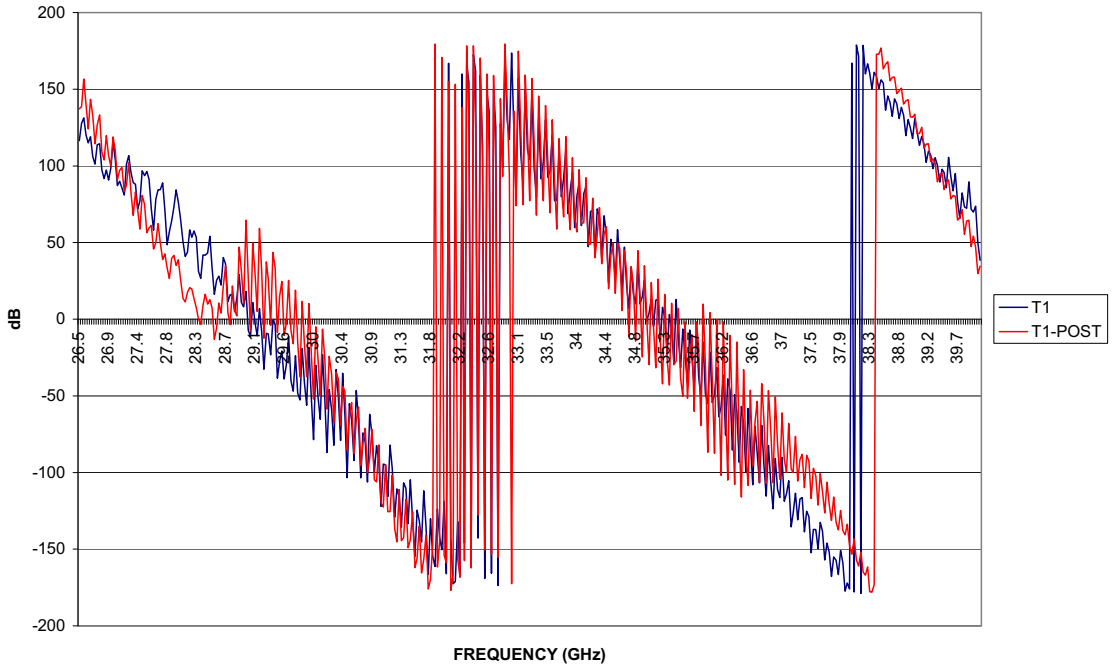

Figure 10 Target 1 Return Loss phase comparison before (blue line) and after (red line) thermal cycling.

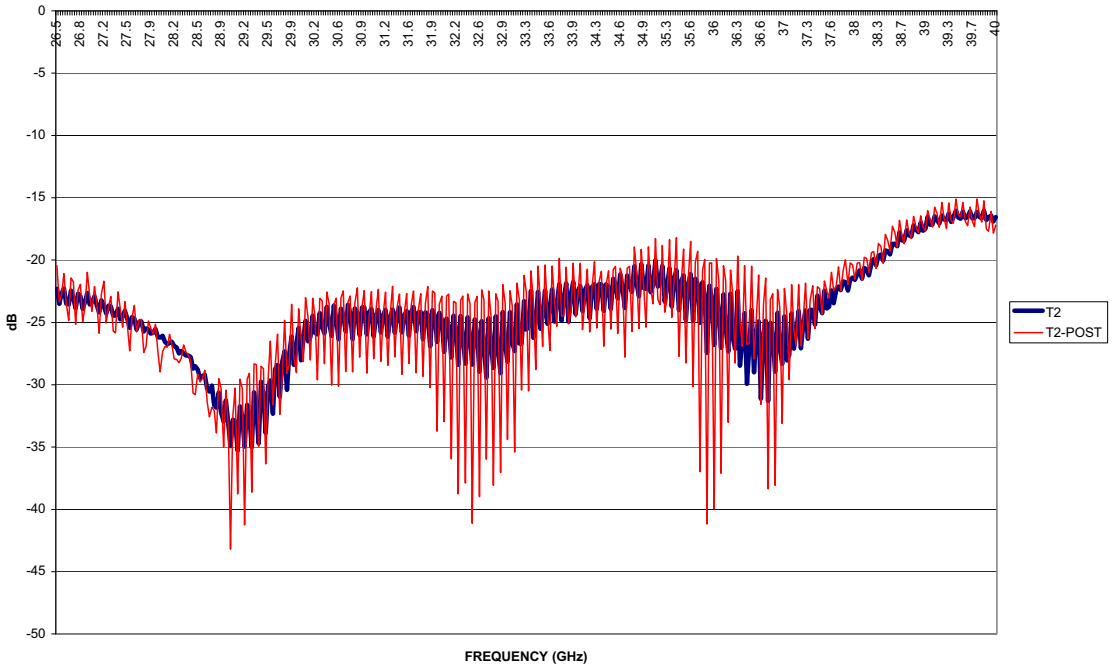

Figure 11 Target 2 Return Loss amplitude comparison before (blue line) and after (red line) thermal cycling.

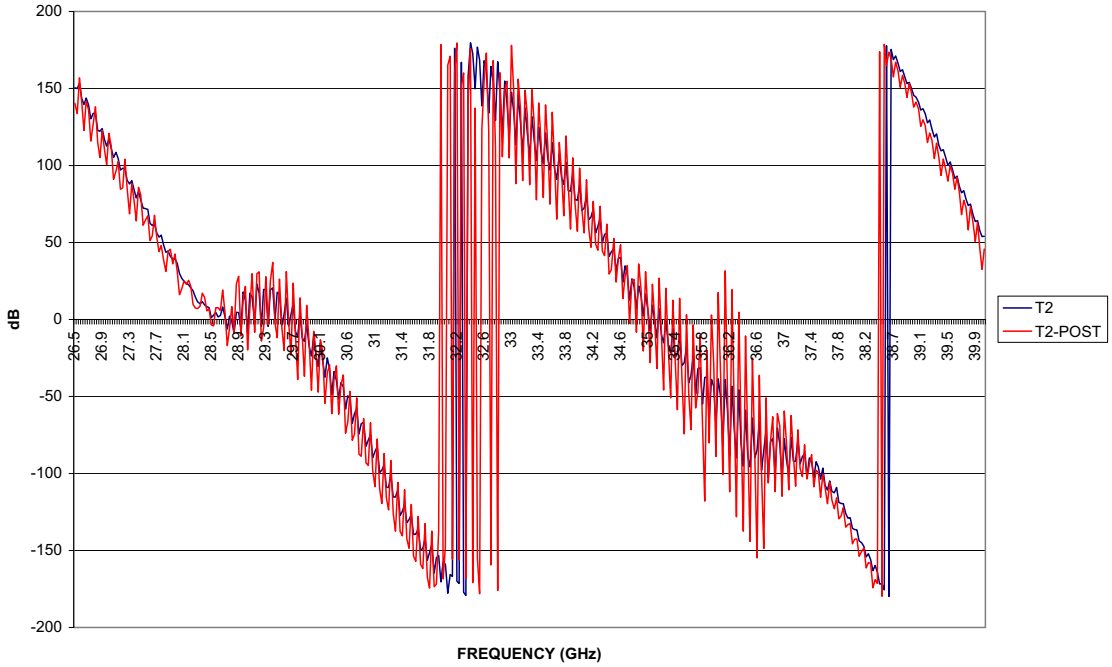

Figure 12 Target 2 Return Loss phase comparison before (blue line) and after (red line) thermal cycling.

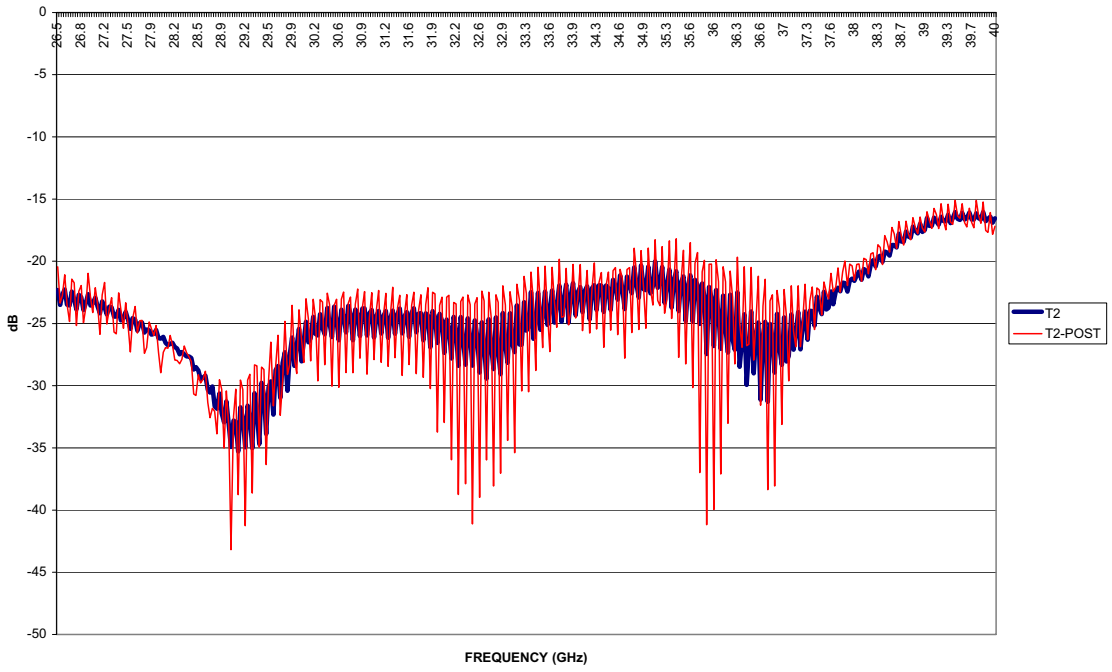

Figure 13 Target 3 Return Loss amplitude comparison before (blue line) and after (red line) thermal cycling.

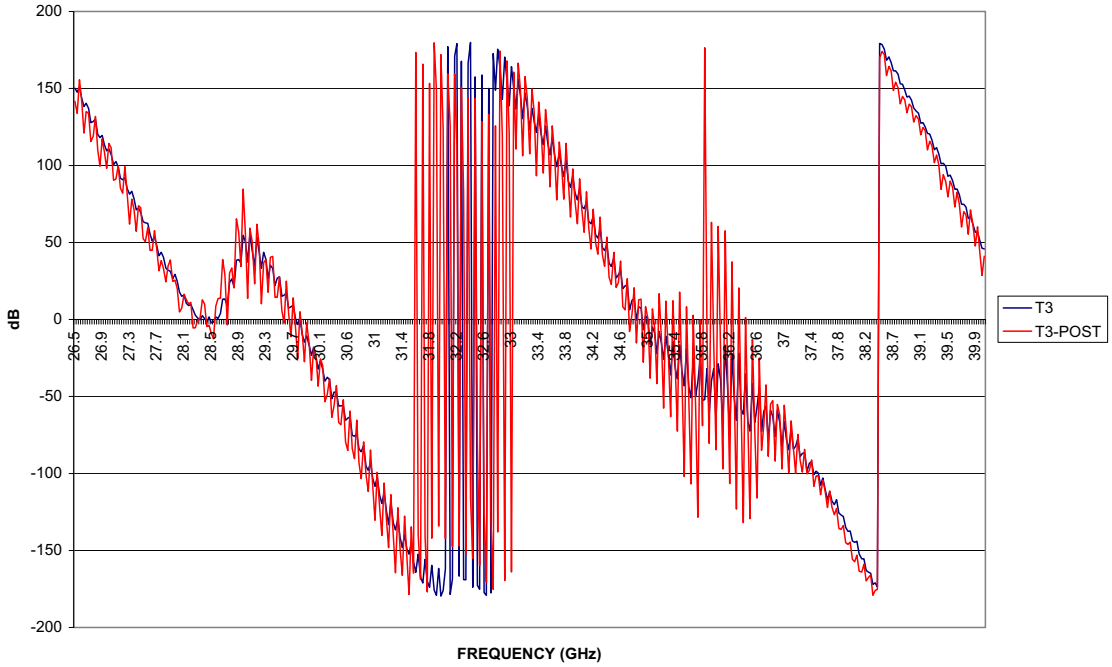

Figure 14 Target 3 Return Loss phase comparison before (blue line) and after (red line) thermal cycling.

Some differences between the data taken before and after thermal cycling are shown in each graph. In particular, all the measurements taken after the thermal cycling are affected by visible ripples growing on the main trace. The shape of the ripples suggests that some difference may be occurred in the radiometric chain between the VNA and the Reference Load. The characteristic frequency of the ripples could help us to determine if some variation has occurred in the load (at distances between 0 mm and about 20 mm from the reflection plane) or if they must ascribed to some variation in the radiometric chain (in the line between the VNA and the Reference Horn mouth).
By performing the Fourier Inverse Transforming of the Return Loss signal (expressed as power) we obtain two characteristic times to be related to characteristic distances from the reflection plane (the horn mouth). The first time give us a characteristic length peaked between 1 mm and 17 mm. The second peak gives a characteristic length peaked between 1 m and 1.5 m. The first peak can be linked to the proper Return loss shape of the trace, due to an impedance mismatching at a distance between 1,5mm (where the Reference Load is placed) and the Reference Load back; the second peak corresponds to the sampling characteristic time (it can not related to any true characteristic time taken from by the radiation to cross the dielectric inside the Reference Load: in fact, being the relative electric permeattivity of the Eccosorb CR110 about 3,5 , the electric length corresponding to this time ranges from 40 to 60 cm). .It does not correspond to any real object causing an increasing reflectivity; its amplitude increases in the last set of measurements. The comparing the two graphs shows that the first peak, tied to the Reference Load characteristics, is very similar in the both cases: this

should mean that no changes in the Reference Load shape or internal structure have influenced the measure.

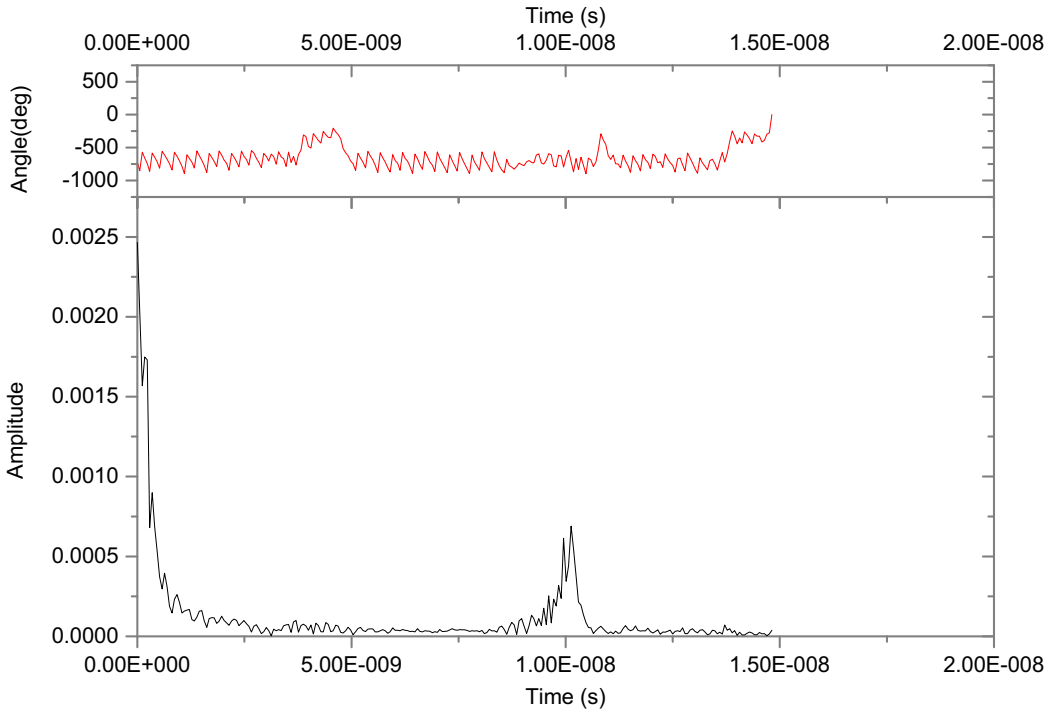

Figure 15 Inverse Fourier Transforming for the T1-Post trace of Figure 9.

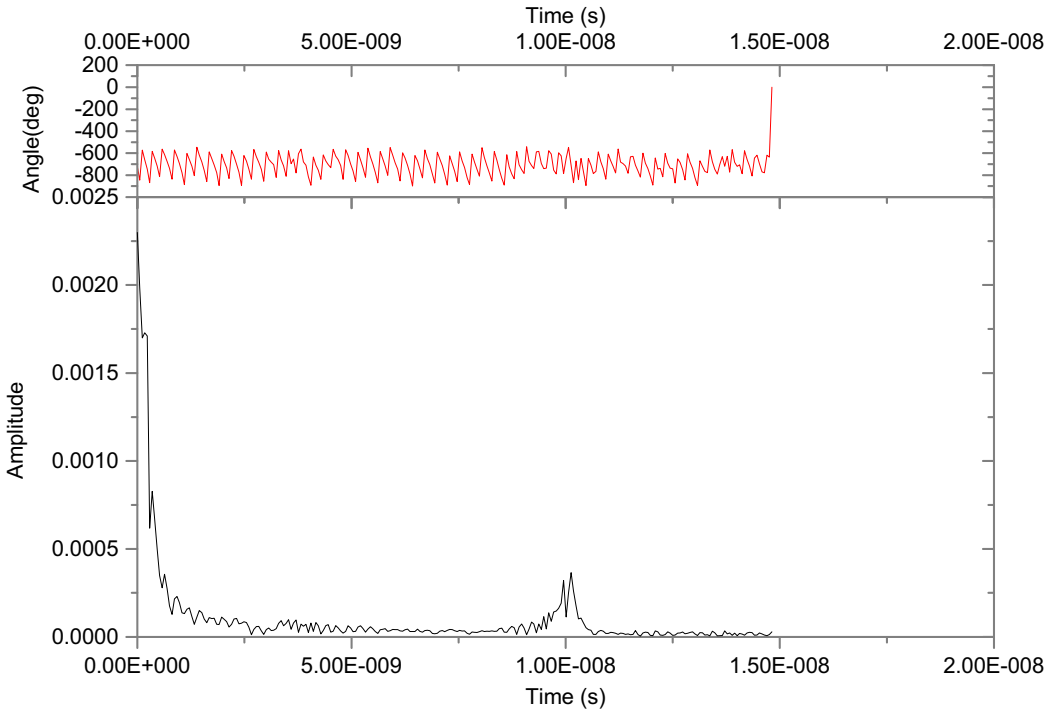

Figure 16 Inverse Fourier Transforming for the T1-trace of Figure 9.

Traces can be smoothed and compared again, making a mobile average of fifth order behaving as a filter. Results follow.

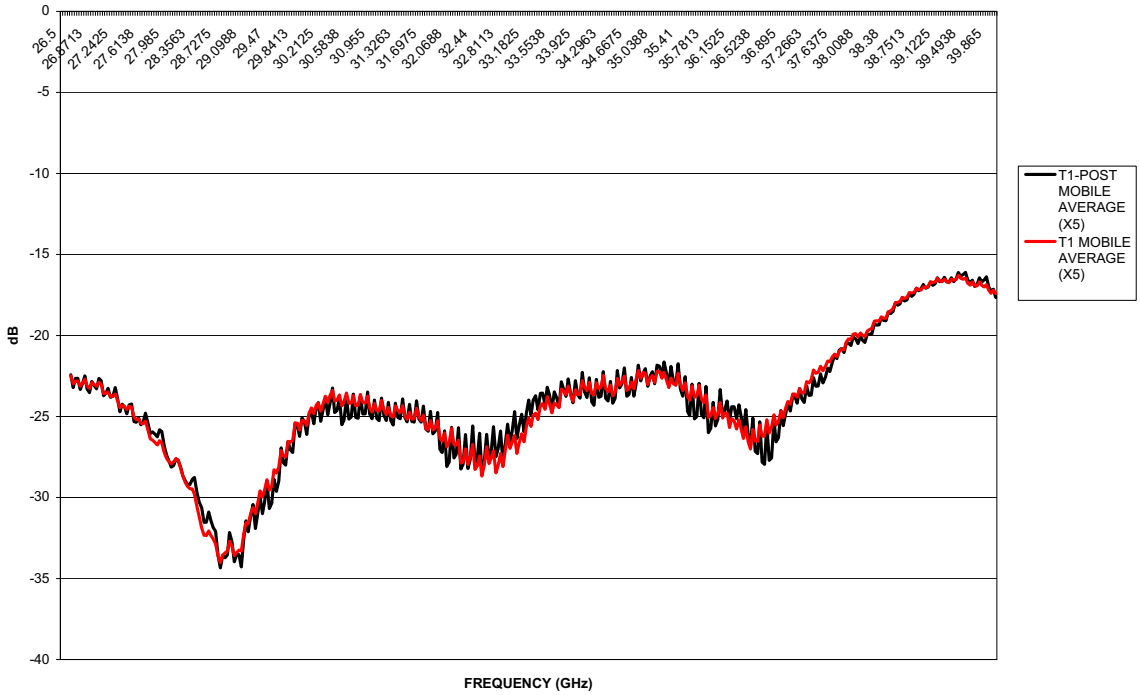

Figure 17 Target 1: comparison of filtered traces

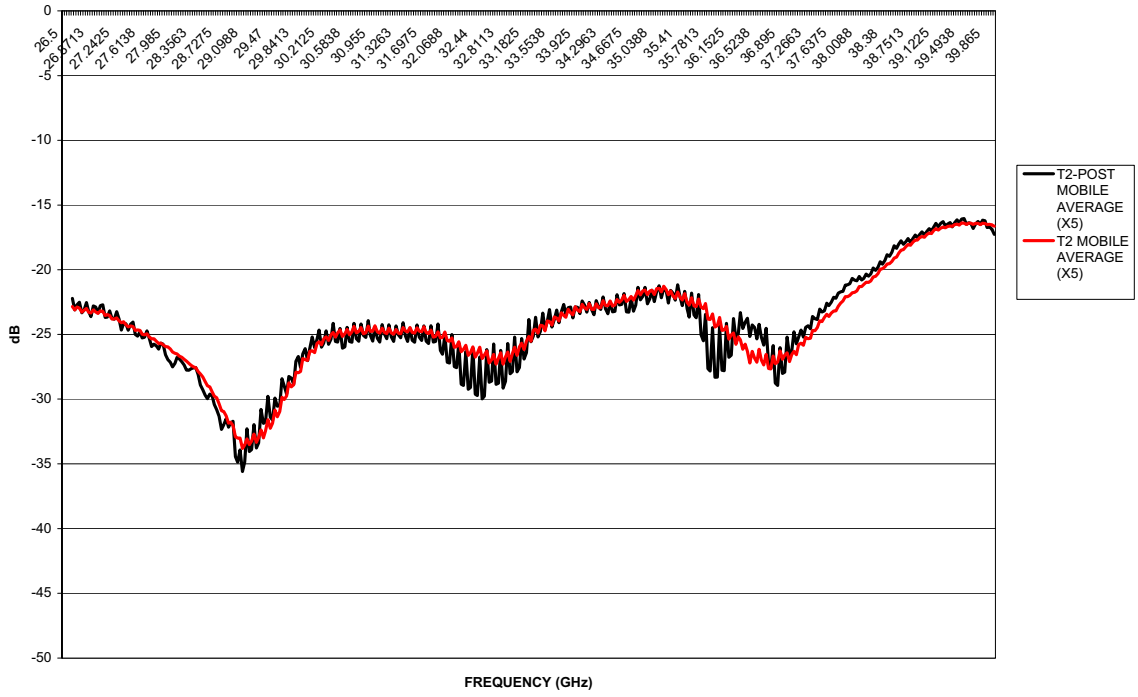

Figure 18 Target 2: comparison of filtered traces

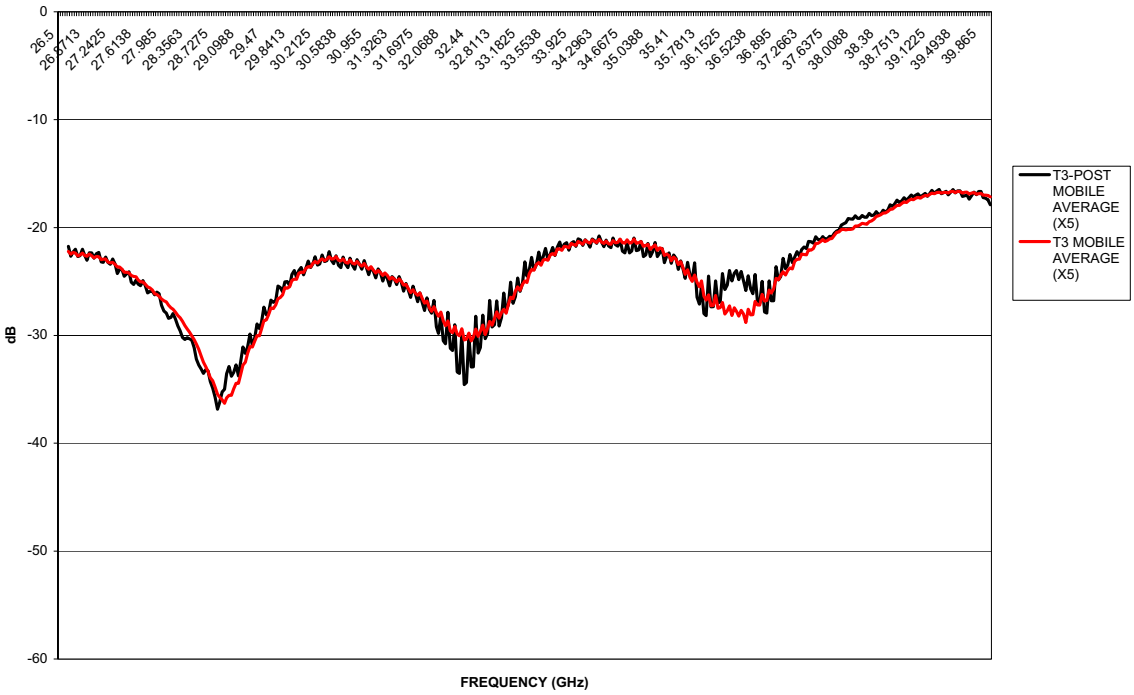

Figure 19 Target 3: comparison of filtered traces

Data shown indicate that none modification has occurred in the Reference Loads T1, T2, T3 structure due to the thermal cycling; differences in the Return Loss amplitude and phase traces are with large probability due to instrumental errors to be linked to a modified calibration between the first and the second measurement.

6.2 WG PL-TES-026 manufacturing RF verification

The part PLTES026 required a mechanical treatment because of some differences with respect to the original design: the waveguide was cut in a specified point, rotated of a 180° angle and joined to the remaining part by using also a connecting waveguide to make safe the original dimensions (the cutting process removes a certain quantity of material changing the total length)

Return Loss and Insertion Loss measurement have been performed on the above part before and after the mechanical treatment, in order to verify the accuracy of the same: in line of principle, a pure 180° rotation of a straight waveguide part around the waveguide axis should not affect much the waveguide impedance (S11); the same reasoning can be extended also to the transmittance (S12).

Return Loss and Insertion Loss plots follow.

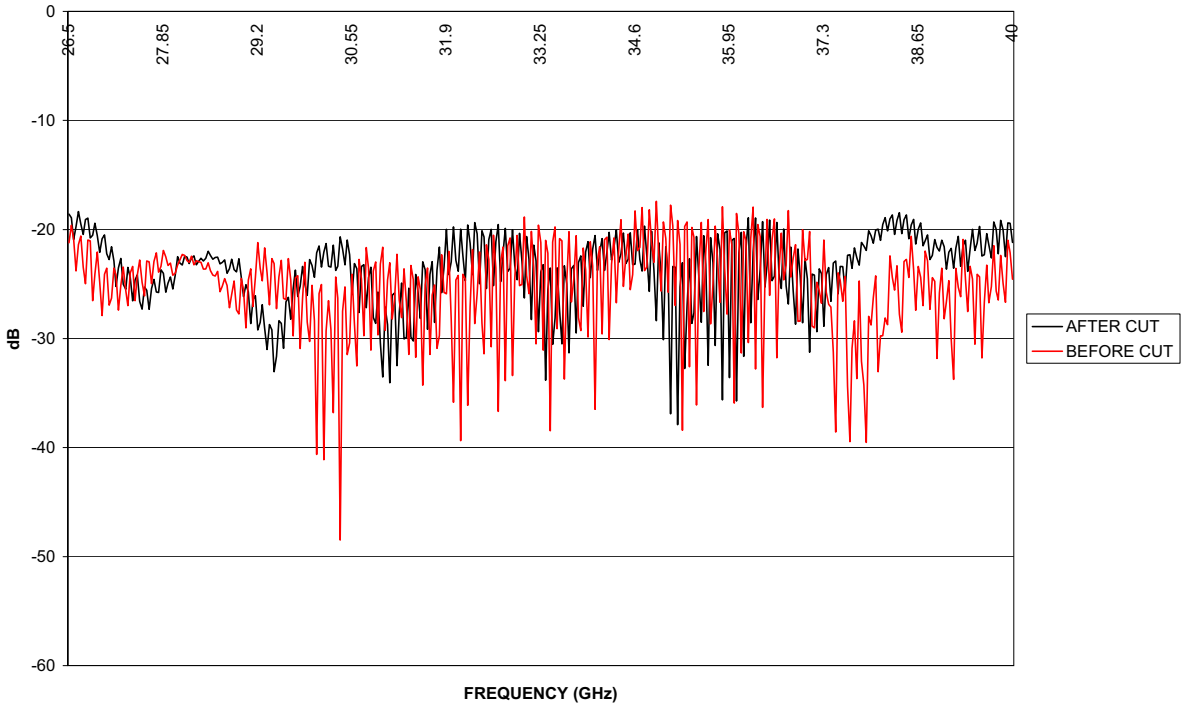

Figure 20 Comparison of Return Loss before (red line) and after (black line) cut

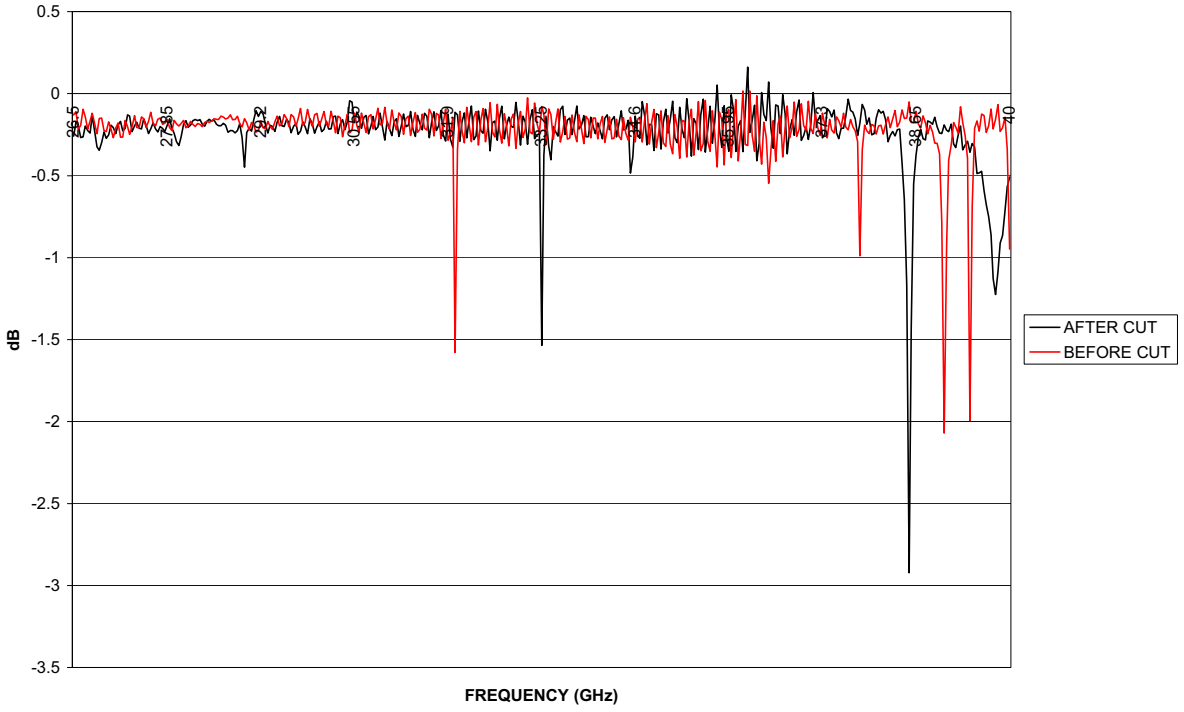

Figure 21 Comparison of Insertion before (red line) and after (black line) cut

AVERAGE INSERTION LOSS:
Before = - 0.21 dB
After = - 0.23 dB

AVERAGE RETURN LOSS:
Before = - 23.67 dB
After = - 22.69 dB

Radiometric performances of the part under investigation changed marginally after the mechanical working. Insertion loss is practically not affected from the treatment, because it depends strongly on the waveguide length. Return loss changes of about 1 dB but it is still largely consistent with requirements.

The part PL-TES-026 was submitted twice to a mechanical working in order to correct a manufacturing error (avoiding the right parallelism between the reference horn and the reference load at the distance of 1,5 mm) but, because of the urgency of integrating it in the RCA facility, it was not possible to test its performances after the last process.

7 RF requirements verification

7.1 Instrumental setup

The VNA is connected to the Reference horn by means of a directional coupler used as holding structure for the antenna. The Reference Load is mounted on a support allowing linear and rotational movements: the positioning can be checked by means of manipulators provided of digital displays having sensibility of 0,001 mm.
The RH-RL alignment is obtained by moving the reference horn left corner and right corner respectively on the left and on the right respect to the RL metal case corners and signing the amount of the displacement; the same operation is repeated by moving up and down over the perpendicular axis.
Insertion Loss measurements are performed by making a Return Loss measurement of the RH terminated by an electrical short (aluminum tape) and dividing by two (since radiation covers a double length) the power lost.
Return Loss measurements are performed by putting the Reference Load in front of the Reference Horn at the nominal distance of 1,5 mm from it.

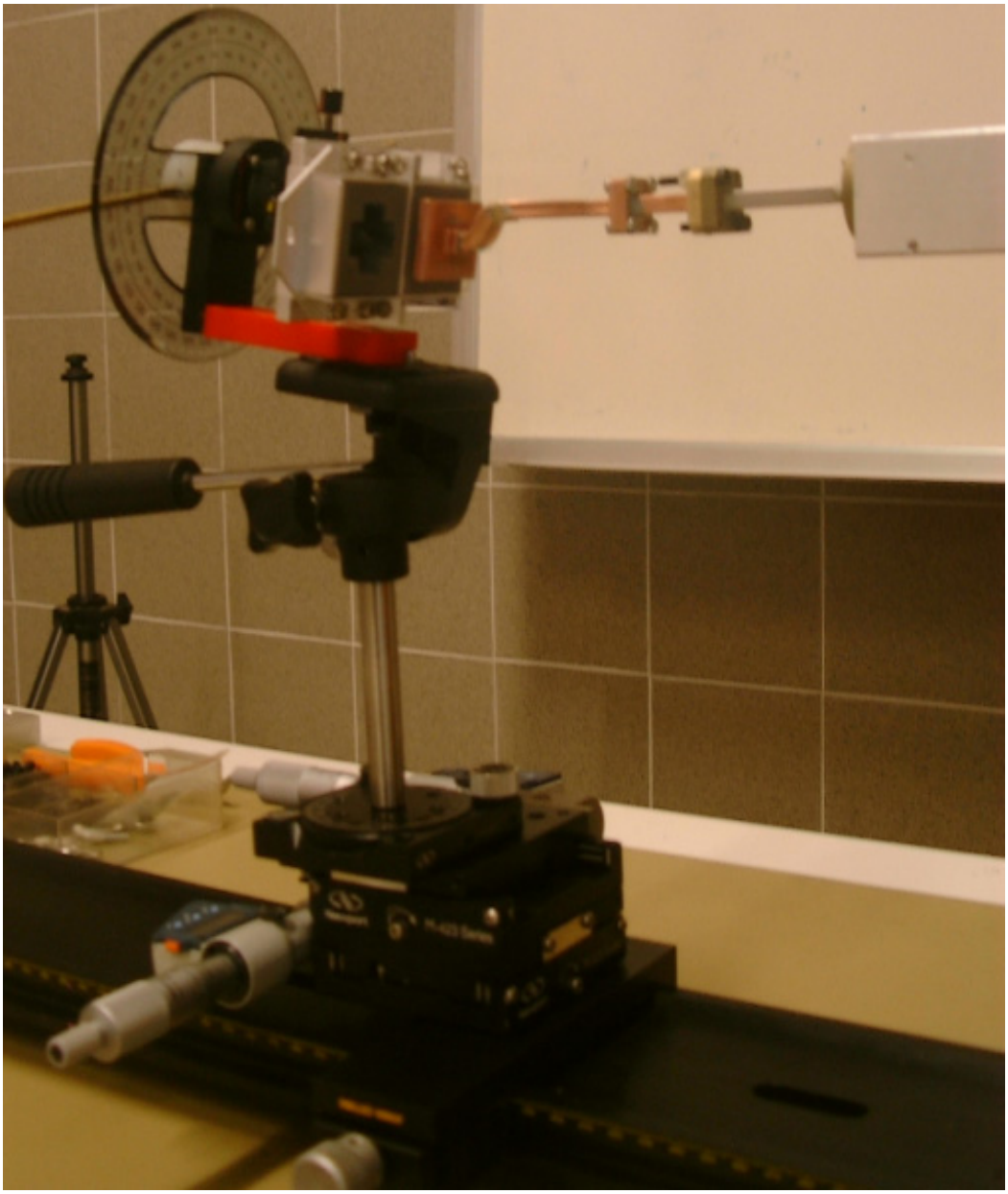

Figure 22 4K reference load mounting structure: the linear and rotational displacement stages, the 4KRL and the feeding reference horn are shown.

7.1.1 Alignment accuracy

Linear displacement stages allow a positioning accuracy of 0,001 mm; angular rotation stages have an accuracy of 1°; However, the angular positioning is checked by means of the linear stages: this trick increases largely the angular position sensibility.

7.2 Insertion Loss measurement

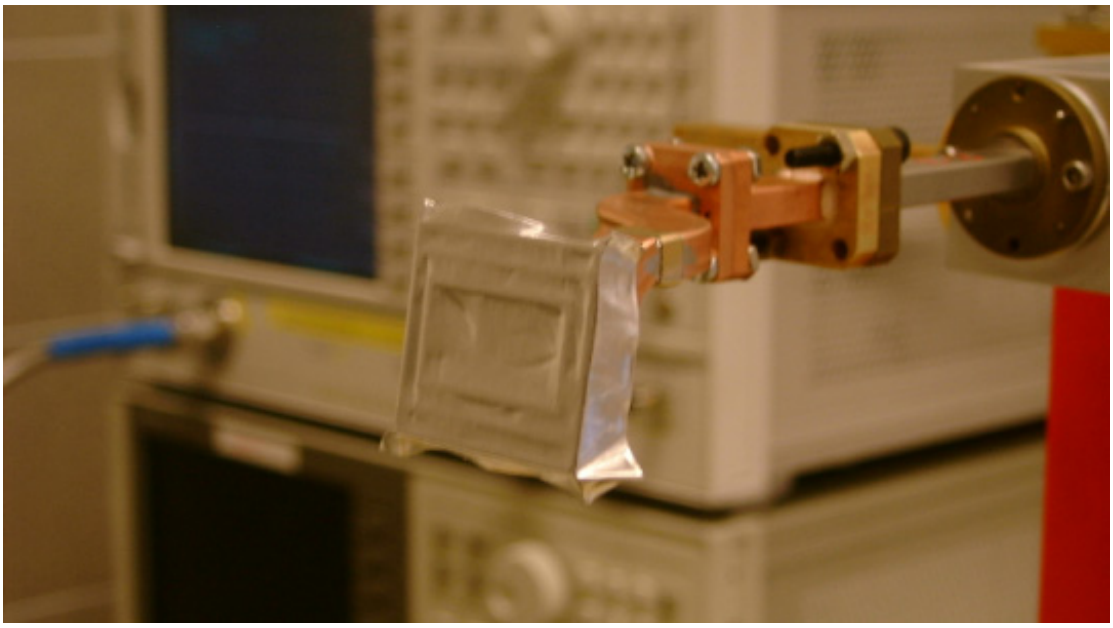

Figure 23 The insertion loss setup is shown: an electrical short (obtained by using an aluminum tape) is mounted on the reference horn mouth. The IL is derived by a RL measurement.

7.2.1 RH 28L

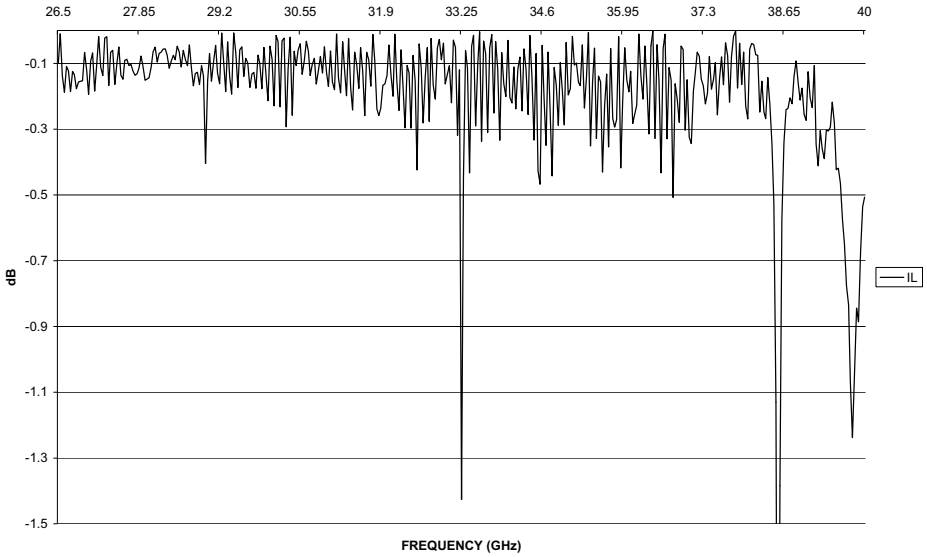

Figure 24 PLTES025L

Il_{eq} [Frequency Range (26,5GHz - 40GHz)]: -0.29 dB
Il_{eq} [Frequency Range (27 GHz - 33GHz)]: -0,26 dB

7.2.2 RH 28R

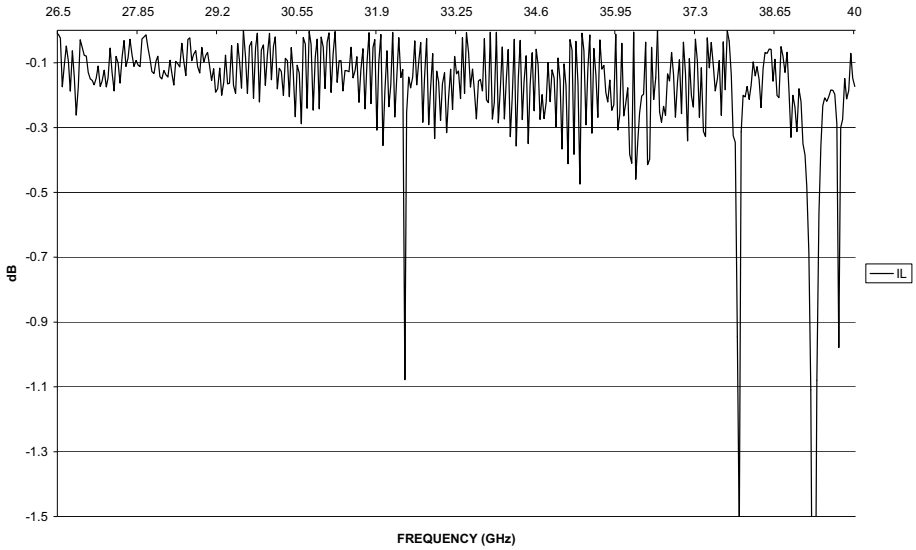

Figure 25 PLTES026R

Il_{eq} [Frequency Range (26,5GHz - 40GHz)]: -0.21 dB
Il_{eq} [Frequency Range (27 GHz - 33GHz)]: -0.18 dB

7.3 Return Loss Measurement

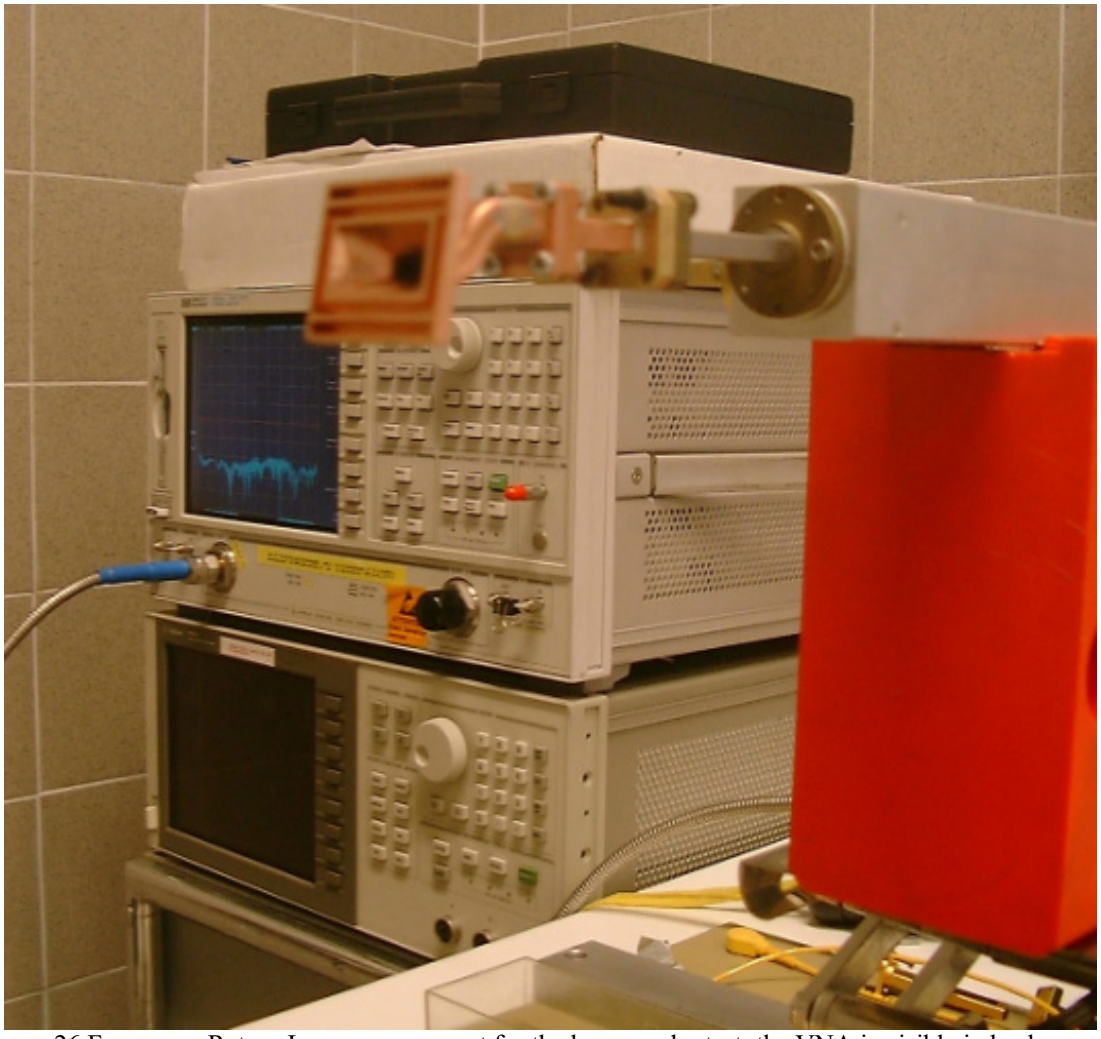

Figure 26 Free space Return Loss measurement for the horns under test; the VNA is visible in background.

7.3.1 RH 28L

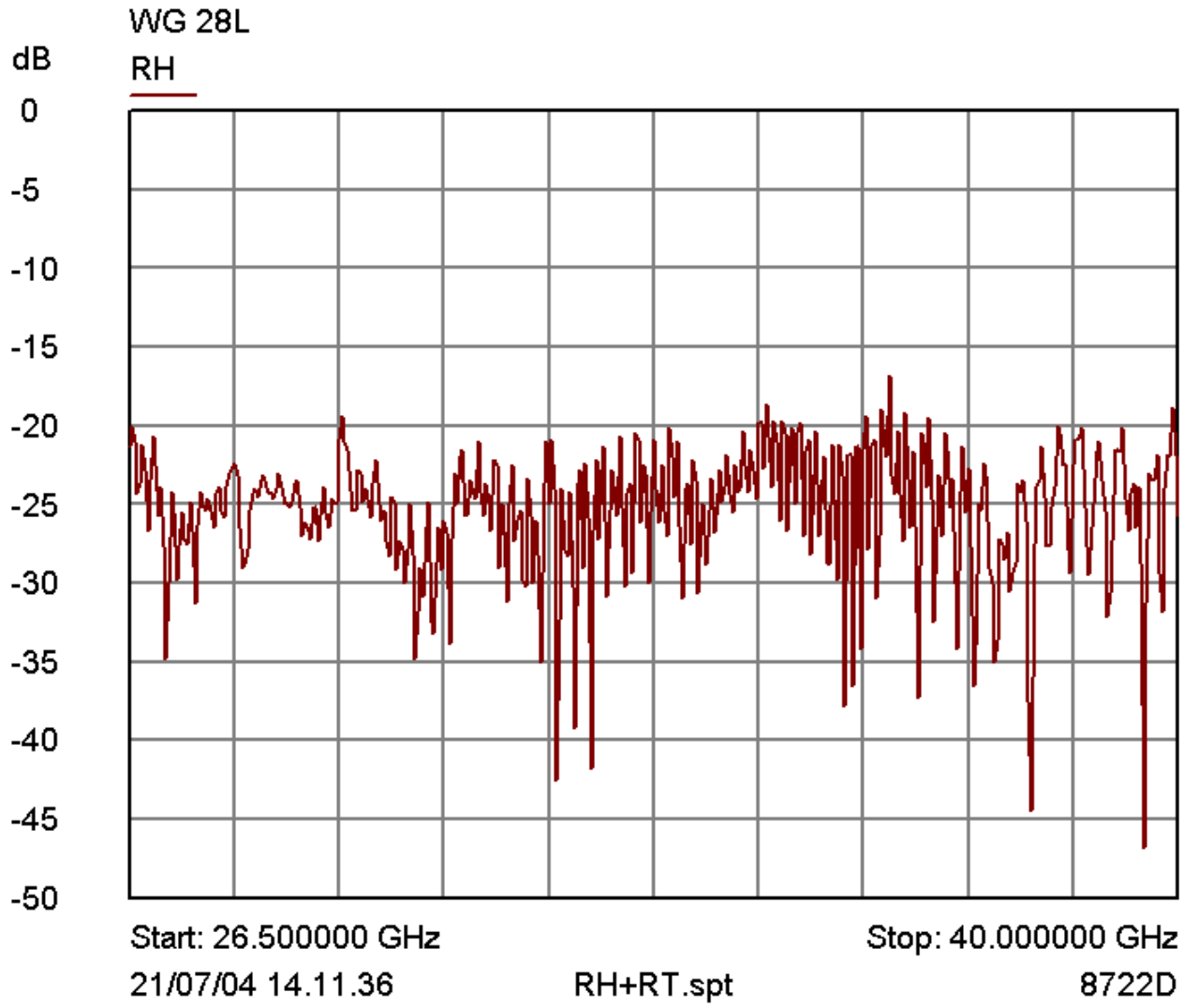

Figure 27 RH 28L return Loss (measured radiating on free space)

Rl_{eq} [Frequency Range (26,5GHz - 40GHz)]: -23.97 dB
Rl_{eq} [Frequency Range (27 GHz - 33GHz)]: -25.00 dB

7.3.2 RH 28R

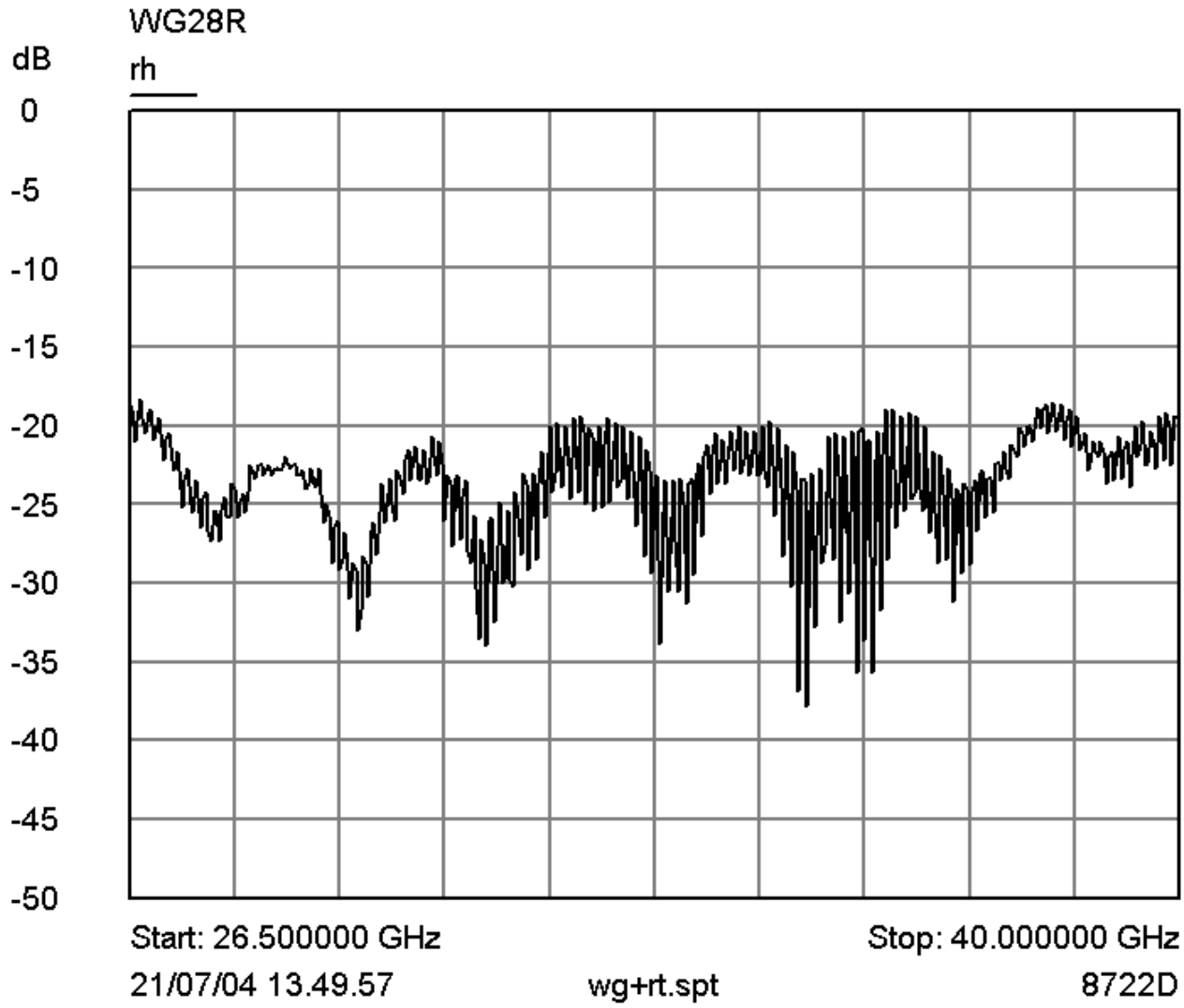

Figure 28 RH 28R return Loss (measured radiating on free space)

Rl_{eq} [Frequency Range (26,5GHz - 40GHz)]: -22.70 dB
Rl_{eq} [Frequency Range (27 GHz - 33GHz)]: -23.70 dB

7.3.3 RH 28L + RT_i

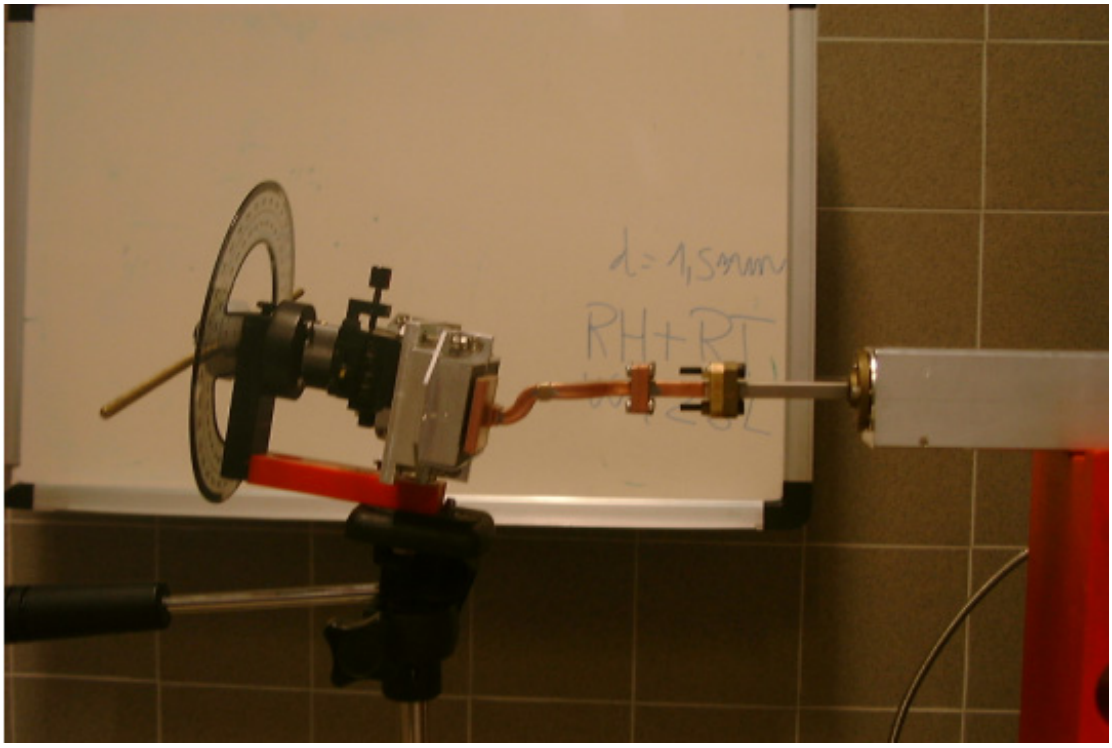

Figure 29 Return Loss of the RH 28L coupled to the three Reference Loads (T1, T2, T3); the RH is put at the nominal distance (1,5 mm) from the RLs.

7.3.3.1 T1

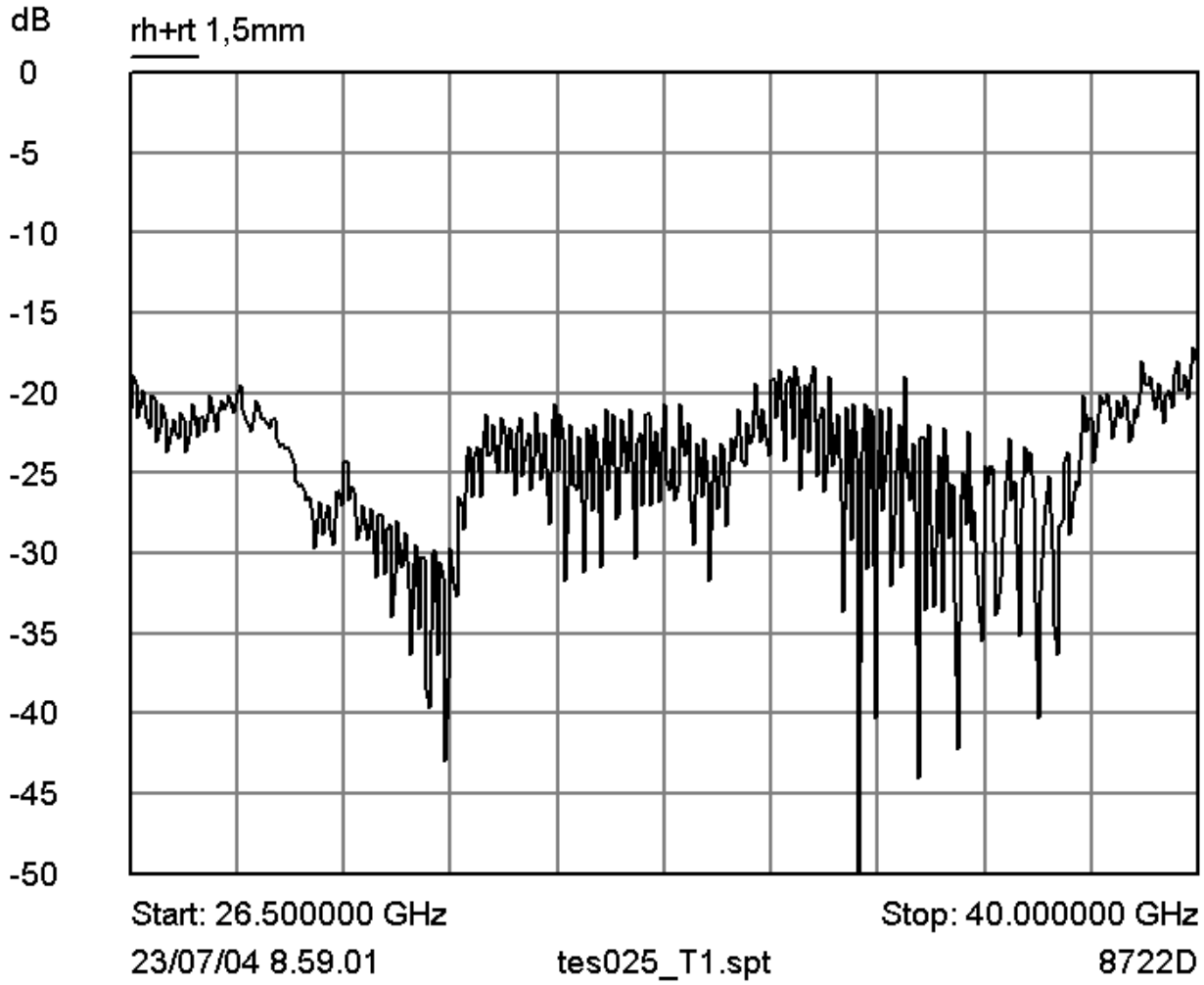

Figure 30 Return Loss of the RH 28L coupled to the Reference Loads T1

Rl_{eq} [Frequency Range (26,5GHz - 40GHz)]: -22.89 dB
Rl_{eq} [Frequency Range (27 GHz - 33GHz)]: -24.06 dB

7.3.3.2 T2

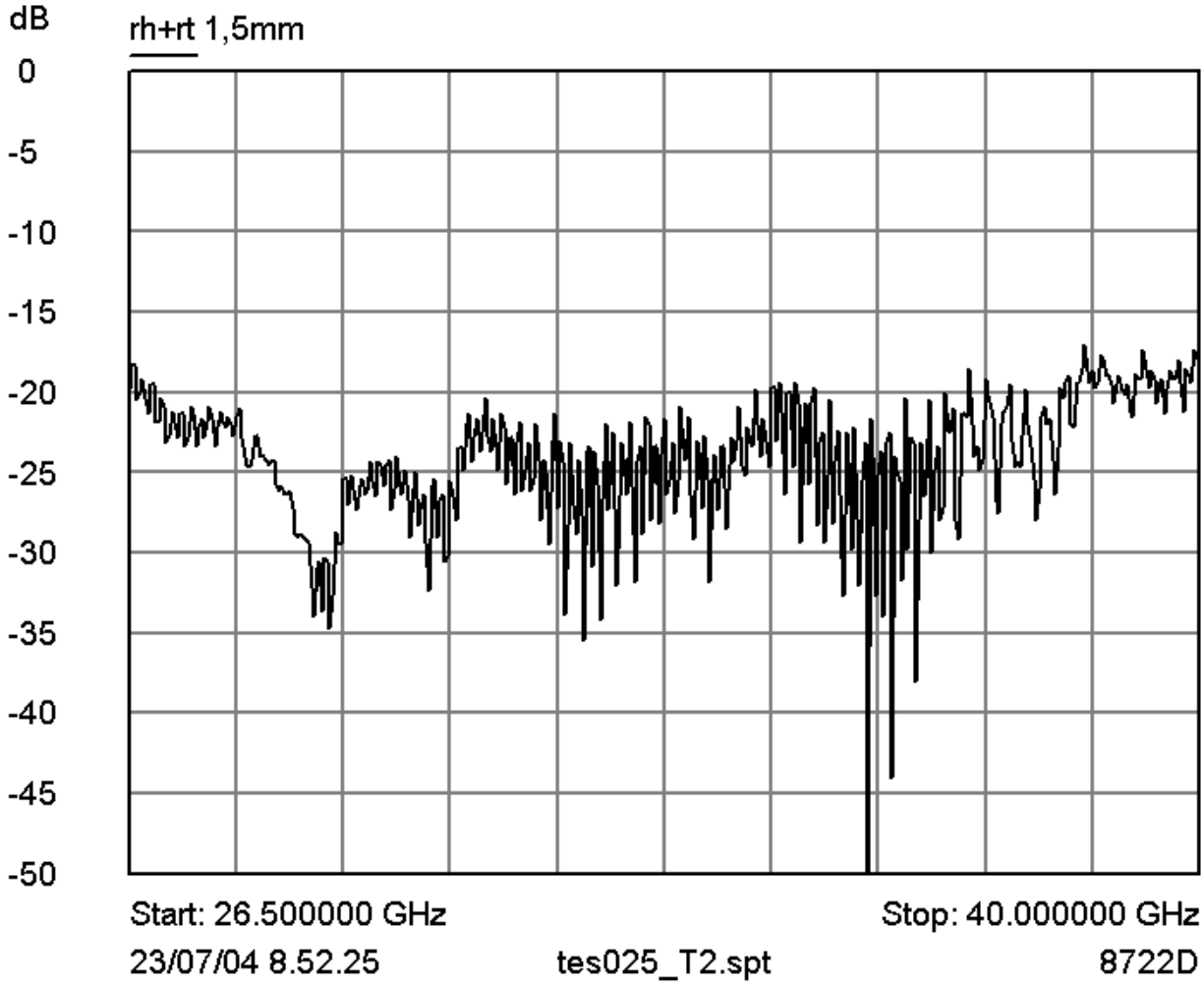

Figure 31 Return Loss of the RH 28L coupled to the Reference Loads T2

Rl_{eq} [Frequency Range (26,5GHz - 40GHz)]: -22.94 dB
Rl_{eq} [Frequency Range (27 GHz - 33GHz)]: -24.62 dB

7.3.3.3 T3

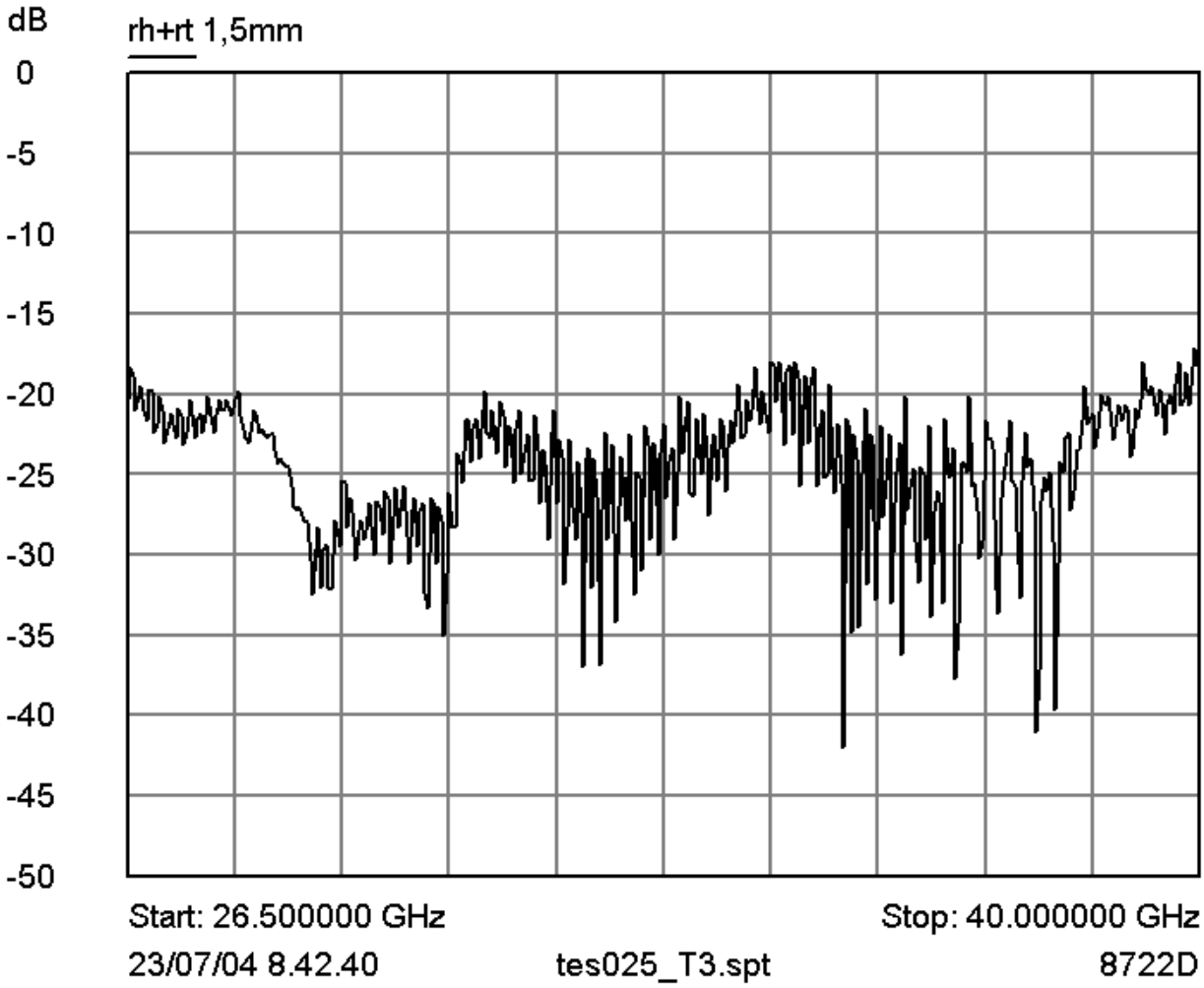

Figure 32 Return Loss of the RH 28L coupled to the Reference Loads T3

Rl_{eq} [Frequency Range (26,5GHz - 40GHz)]: -23.00 dB
Rl_{eq} [Frequency Range (27 GHz - 33GHz)]: -24.29 dB

7.3.4 RH 28R + RT_i

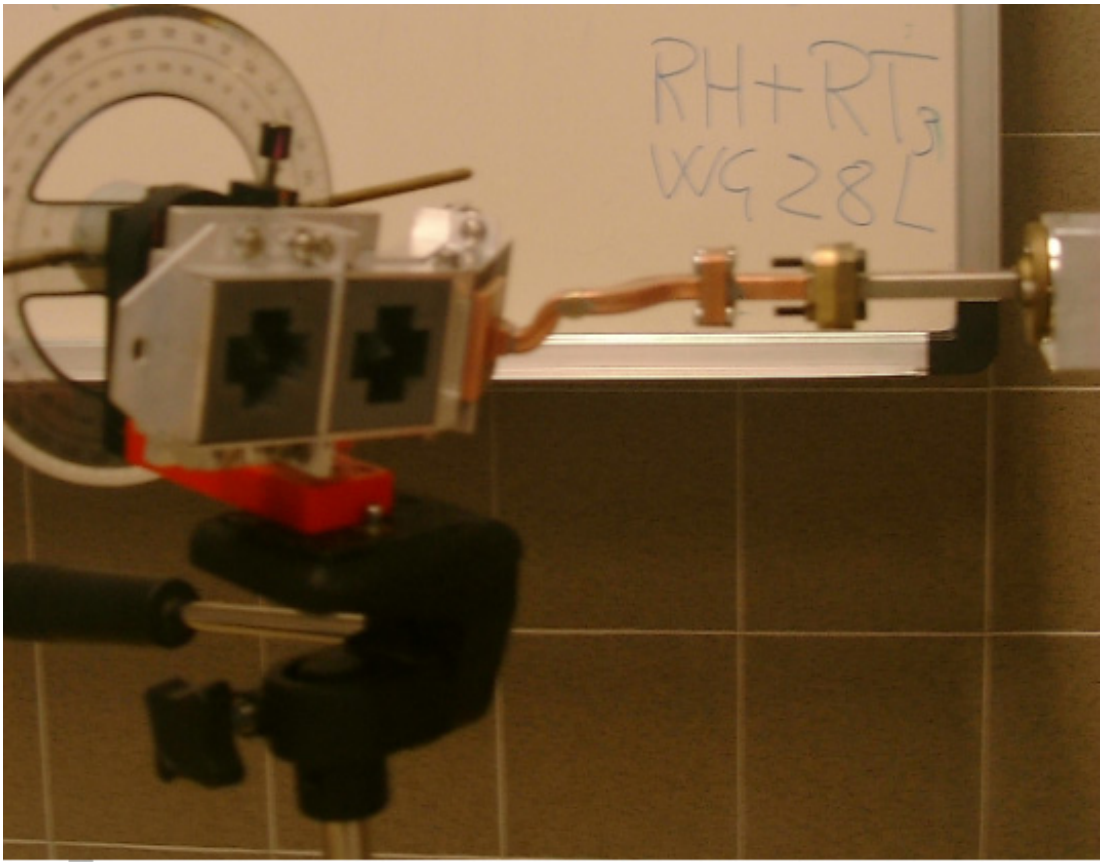

Figure 33 Return Loss of the RH 28R coupled to the three Reference Loads (T1, T2, T3); the RH is put at the nominal distance (1,5 mm) from the RLs.

7.3.4.1 T1

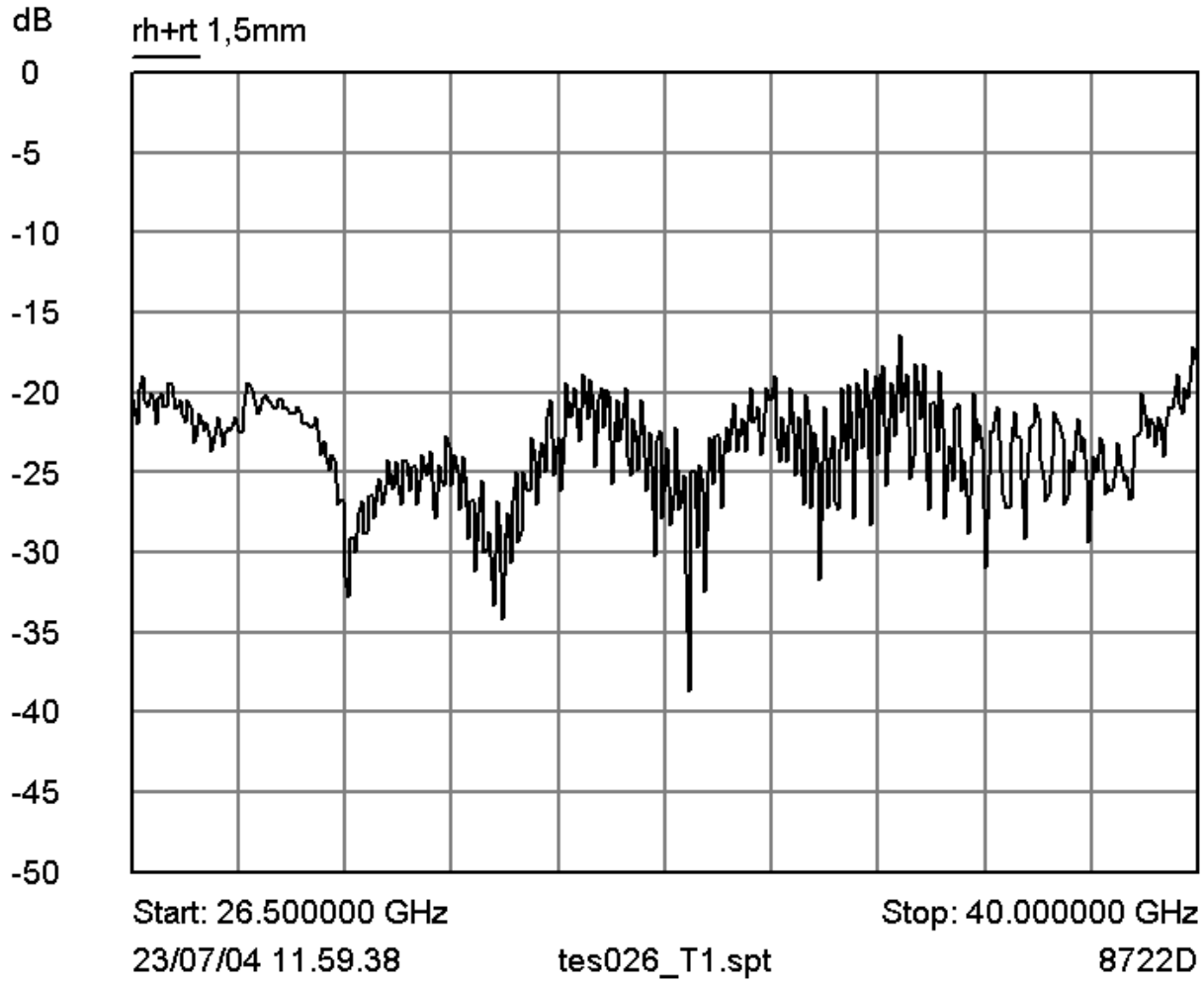

Figure 34 Return Loss of the RH 28R coupled to the Reference Loads T1

Rl_{eq} [Frequency Range (26,5GHz - 40GHz)]: -22.71 dB
Rl_{eq} [Frequency Range (27 GHz - 33GHz)]: -22.95 dB

7.3.4.2 T2

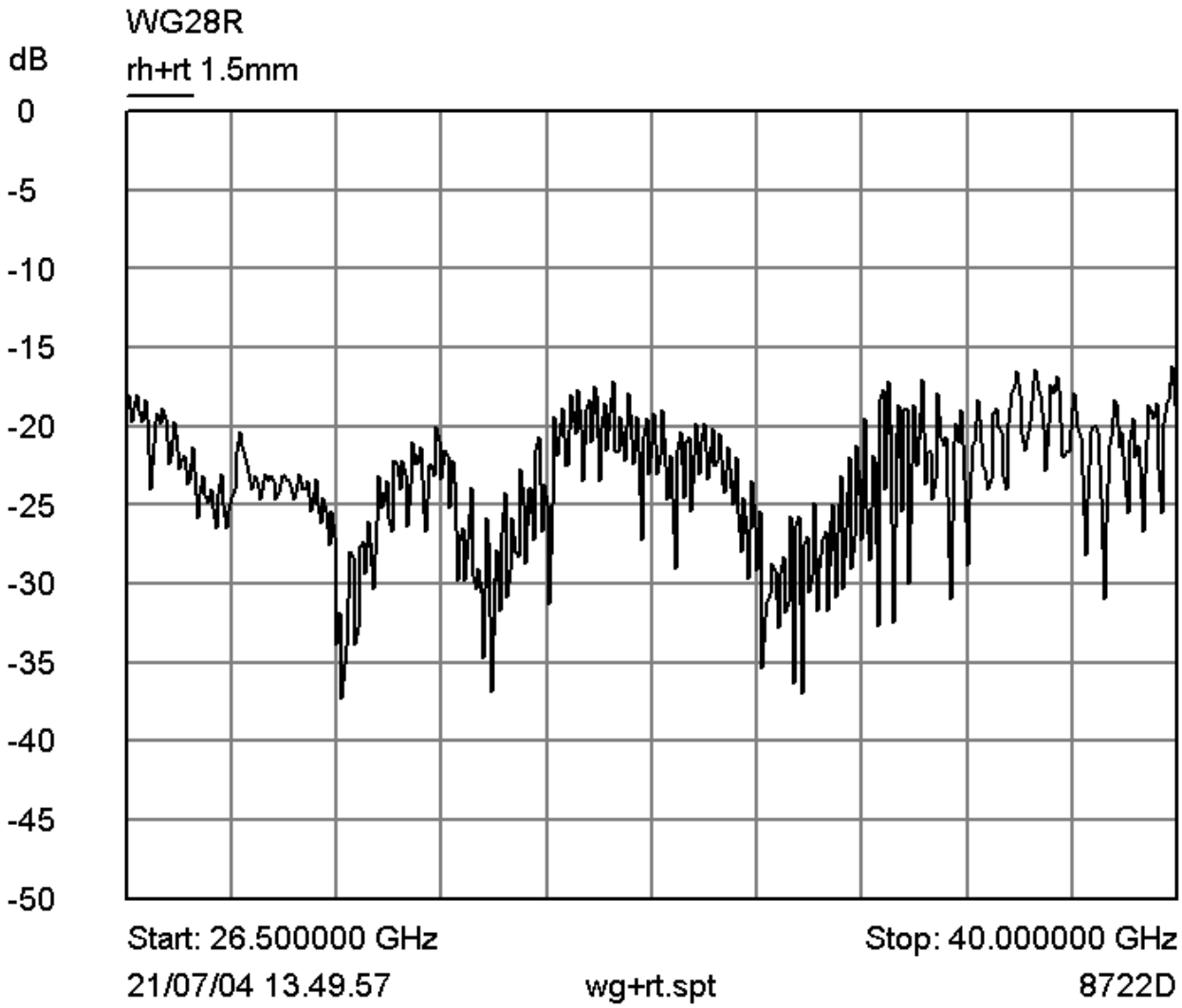

Figure 35 Return Loss of the RH 28R coupled to the Reference Loads T2

Rl_{eq} [Frequency Range (26,5GHz - 40GHz)]: -22.84 dB
Rl_{eq} [Frequency Range (27 GHz - 33GHz)]: -23.85 dB

7.3.4.3 T3

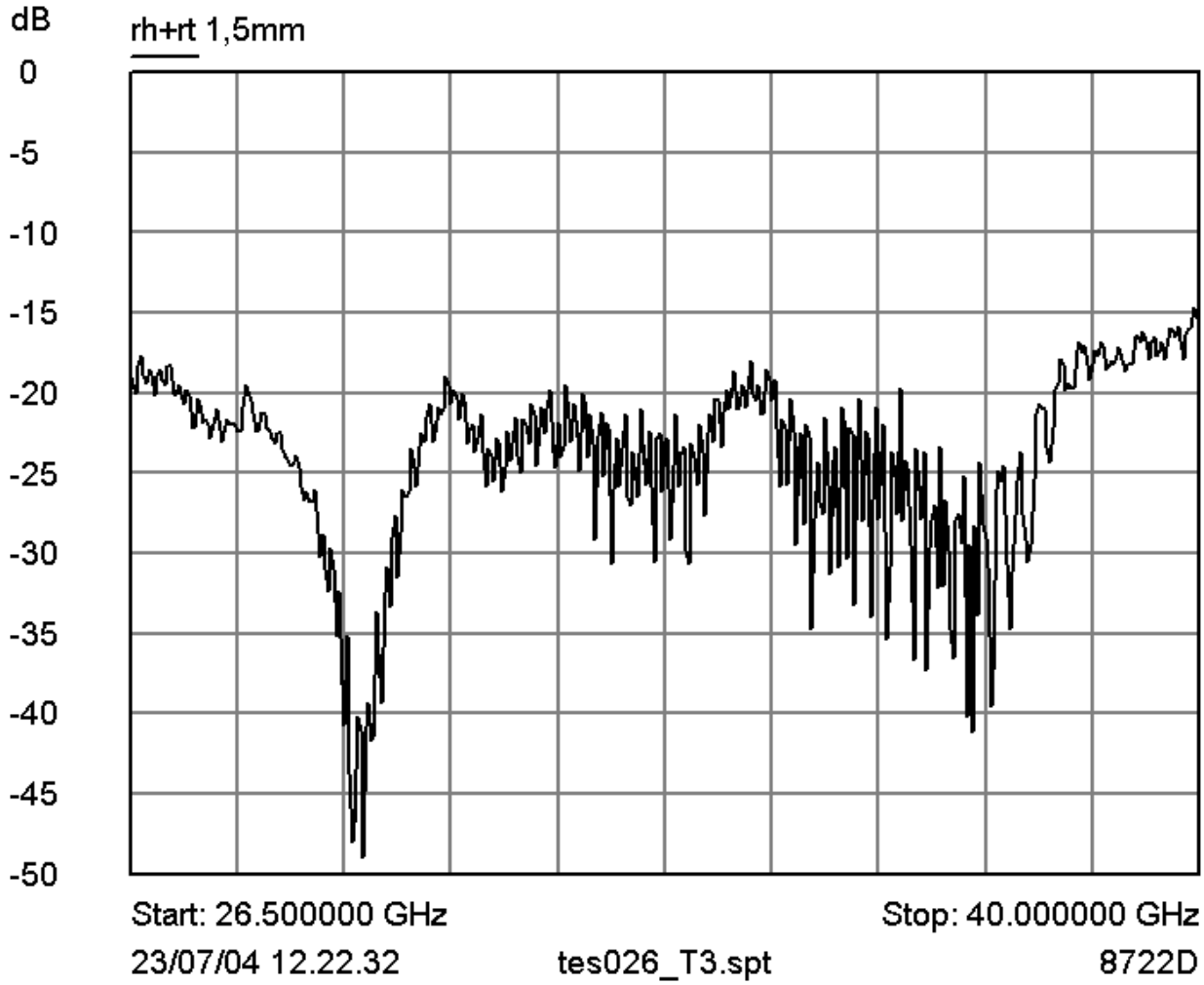

Figure 36 Return Loss of the RH 28R coupled to the Reference Loads T3

Rl_{eq} [Frequency Range (26,5GHz - 40GHz)]: -22.66 dB
Rl_{eq} [Frequency Range (27 GHz - 33GHz)]: -23.07 dB

8 RF RESULTS AND DATA ANALYSIS

For each test reported above the average value in two operational ranges has been evaluated: in fact since the flight radiometers integrate the power detected over the full band, we use, as representative parameter defining the quantity to be measured, the average power over the whole band, expressed in dB.

For the reflectivity of the RH-RL system and of the RH alone radiating in free space it is the Equivalent Return Loss; to represent the power loss in the waveguide-Reference horn system it is the Equivalent Insertion Loss.

EQ[1]
$$RL_{eq} = 10 \times LOG \frac{\int P_{refl}\, d\nu}{\Delta\nu} = 10 \times LOG \frac{\sum_{i=1}^{n} \left[(S_{22})^2\right]_i}{n}$$

EQ[2]
$$IL_{eq} = 10 \times LOG \frac{\int P_{trasm}\, d\nu}{\Delta\nu} = 10 \times LOG \frac{\sum_{i=1}^{n} \left[(S_{12})^2\right]_i}{n}$$

Two frequency ranges have been considered in order of verifying performances also out of the nominal 20% frequency band.

Results, for the whole set of tests are represented in terms of equivalent power in the following histograms: each histogram displays simultaneously the results obtained for the two parts under test (RH28L, ID PLTES025 and RH28R, ID PLTES026) in the two frequency ranges.

8.1 RH-RL Equivalent Return Loss

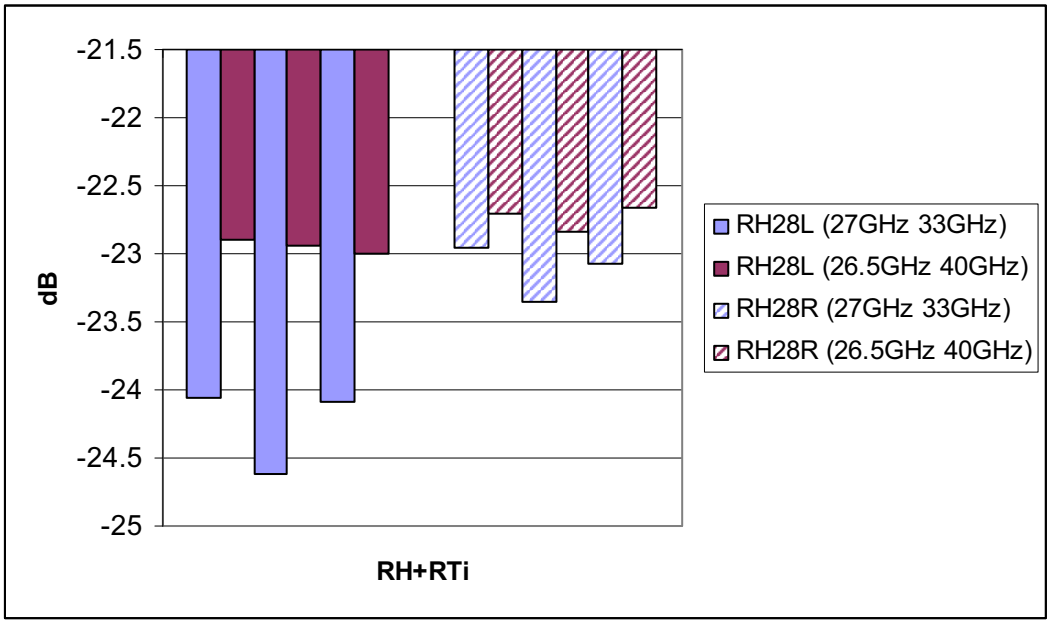

Plot 1 Equivalent Return Loss comparison between the two reference horns under test (28l and 28R); two range of frequencies have been considered (26,5-40 GHz and 27-33 GHz): each horn have been tested coupled to each of the three reference targets (T1 T2 T3 corresponding to the first, second and third column of the same color) (the combination of RH and RL inside the RCA: RH28L+T1, RH28R+T2)

8.2 RH Equivalent Return Loss

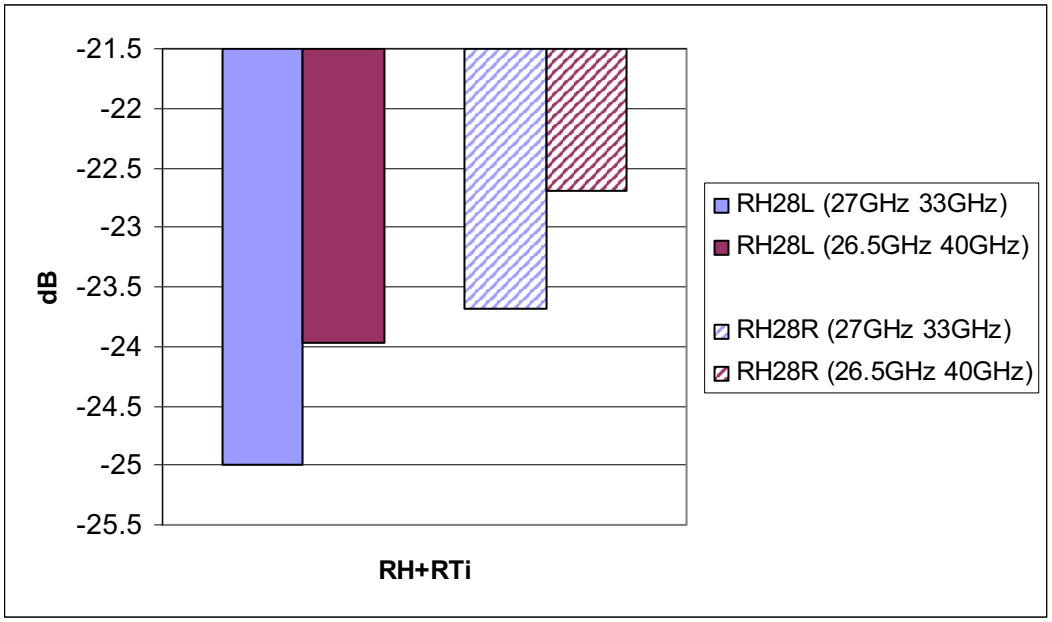

Plot 2 Equivalent Return Loss comparison between the two reference horns under test (28l and 28R); two range of frequencies have been considered (26,5-40 GHz and 27-33 GHz)

8.3 RH Equivalent insertion Loss

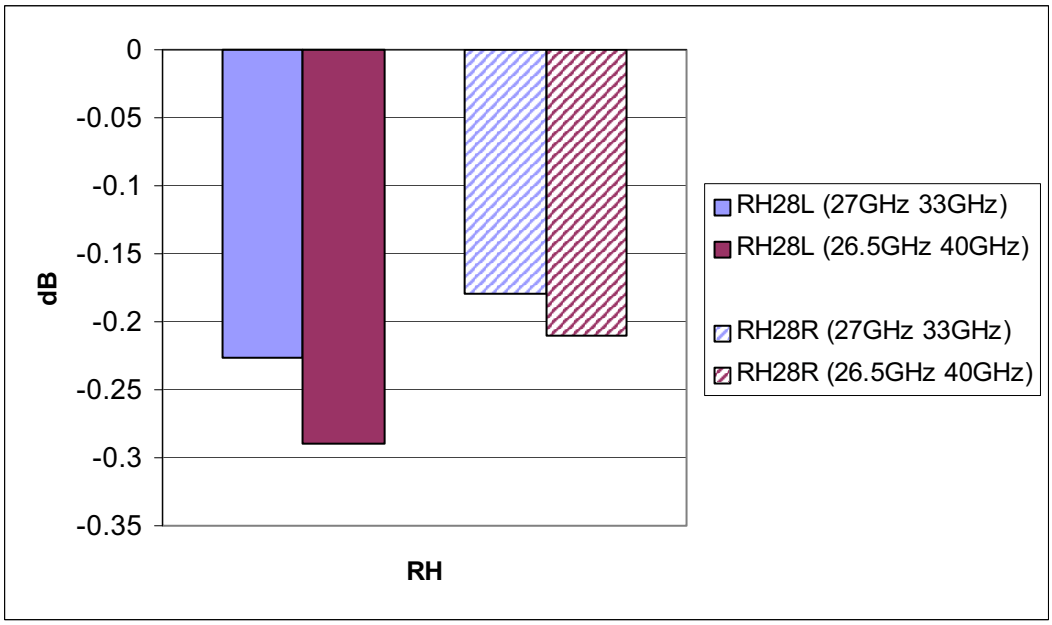

Plot 3 Equivalent insertion Loss comparison between the two reference horns under test (28l and 28R); two range of frequencies have been considered (26,5-40 GHz and 27-33 GHz)

8.4 Data analysis and comparison with requirements

From results shown above some features can be outlined:

a) The Return loss is quite similar for the four Reference horns (comprising the RH and Reference waveguide) tested: a little performance improving is registered for the RH28L: this feature reflects also on a better matching with the Reference Loads.

b) The Insertion Loss is quite similar in the both parts tested.

c) the differences between the three reference loads, tested using the same RH, is negligible: it is less than 0,5 dB and can be ascribed also to the different position that each RL occupies inside the Reference Case (in fact differences follow the same behaviour for the both Reference Horns tested, as displayed by Plot 1.

d) Requirements (REF[3]) stated for the Equivalent Return Loss a level lower than –20dB and for the Equivalent Insertion Loss higher than –1dB; both the Reference Horns under test, also coupled to the three Reference Loads, satisfy the requirements. Tests have been performed coupling each RH to each one of the three reference Loads; however is to be considered that the combination required for the Qualification Model are only the:

   PL-TES-025 + T1
   PL-TES-026 + T2

e) Performances of the part subjected to the mechanical working (PL-TES-025) seems to be not affected from it. However, it is to be considered that a second mechanical treatment was performed later and that the final part was not tested again.

9 CONCLUSIONS

The parts delivered to Laben S.p.a. to be assembled inside the RCA cryo facility have been characterised from the thermal and radiometric point.
Two thermal cycling processes (complete cool down and warm up) were performed on the reference loads to test their resistance to thermal shocking. The visual inspection did not get any indication of damage.
Radiometric verification was been performed before and after the thermal cycling to verify if some permanent change in RF behaviour (due to some modification in the material structure not evidenced by visual inspection) is produced by the cooling: it did not produce any evidence of changing.
The dimensional design was verified: some deviation from nominal values was registered and outlined.
The agreement with radiometric requirements was verified: single parts and the complete systems agree with requirements indicated in REF[3] Only a part (PL-TES-025) was not

tested in its final design and delivered to Laben without being certified, because of schedule needs.